The Astronomical Journal, 124:3404–3423, 2002 December

FORMATION OF THE GALILEAN SATELLITES: CONDITIONS OF ACCRETION

Robin M. Canup and William R. Ward
Department of Space Studies, Southwest Research Institute, 1050 Walnut Street, Suite 400, Boulder, CO 80302;
robin@boulder.swri.edu
Received 2002 June 17; accepted 2002 September 9

ABSTRACT

We examine formation conditions for the Galilean satellites in the context of models of late-stage giant planet accretion and satellite-disk interactions. We first reevaluate the current standard, in which the satellites form from a "minimum mass subnebula" disk, obtained by augmenting the mass of the current satellites to solar abundance and resulting in a disk mass containing about 2% of Jupiter's mass. Conditions in such a massive and gas-rich disk are difficult to reconcile with both the icy compositions of Ganymede and Callisto and the protracted formation time needed to explain Callisto's apparent incomplete differentiation. In addition, we argue that disk torques in such a gas-rich disk would cause large satellites to be lost to inward decay onto the planet. These issues have prevented us from identifying a self-consistent scenario for the formation and survival of the Galilean satellites using the standard model. We then consider an alternative, in which the satellites form in a circumplanetary accretion disk produced during the very end stages of gas accretion onto Jupiter. In this case, an amount of gas and solids of at least $\sim$0.02 Jovian masses must still be processed through the disk during the satellite formation era, but this amount need not have been present all at once. We find that an accretion disk produced by a slow inflow of gas and solids, e.g., 2×10^{-7} Jovian masses per year, is most consistent with conditions needed to form the Galilean satellites, including disk temperatures low enough for ices and protracted satellite accretion times of $\geq 10^5$ yr. Such a "gas-starved" disk has an orders-of-magnitude lower gas surface density than the minimum mass subnebula (and for many cases is optically thin). Solids delivered to the disk build up over many disk viscous cycles, resulting in a greatly reduced gas-to-solids ratio during the final stages of satellite accretion. This allows for the survival of Galilean-sized satellites against disk torques over a wide range of plausible conditions.

Key words: planets and satellites: formation — solar system

1. INTRODUCTION AND BACKGROUND

The Galilean satellites have played an influential role in planetary science, from helping to establish the Copernican view of the solar system, to displaying a myriad of physical characteristics and intriguing dynamical and chemical histories. At Jupiter is a satellite system worthy of the term "a mini solar system," whose origin may provide us with insights into planetary formation processes, in particular those involving the growth of gas giant planets.

In this work, we address the formation of the Galilean satellites in the context of an improved understanding of both Jovian accretion and the nature of satellite-disk interactions. Previous works have assumed a gas-rich protosatellite disk containing about 2% of Jupiter's mass—the mass of the current satellites augmented to solar composition, or a "minimum mass subnebula," in direct analogy to the planetary "minimum mass nebula" (see Fig. 1, from Pollack & Consolmagno 1982). However, we show in § 2 that predicted conditions in such a high surface density disk are difficult to reconcile with the characteristics of the satellites themselves, especially when the effects of satellite-disk interactions are included (e.g., Ward & Canup 2002). Indeed, we are unable to construct a simple and self-consistent scenario for the formation and survival of the Galilean satellites in such a "gas-rich" disk model.

We then consider an alternative view in § 3. Although the current satellites imply a lower limit $\sim 0.02 M_J$ for the mass processed through the circumjovian disk during the satellite formation era, all need not have been present in the disk at any one time. By analogy to mineral deposits in a pipe—whose thickness is indicative of the total amount of water slowly processed through the pipe, rather than the total volume contained in the pipe at any one moment—a circumjovian disk supplied by a slow inflow of nebular gas could have had an instantaneous disk mass much less than that of the minimum mass subnebula, but so long as the disk existed for multiple disk supply cycles, a buildup of an appropriate total mass in solids could occur. The satellites would then form more slowly, and in a less gas-rich environment. Preliminary calculations (Canup & Ward 2002a) suggested that this model held promise for simultaneously accounting for several key constraints, including the varying ice/rock content of the satellites, a partially differentiated Callisto, and satellite survival against orbital decay. Stevenson (2001) independently reasoned that such a scenario—which he referred to as the "gas-starved" disk model, a name we adopt here—might provide an attractive alternative. Here we demonstrate that conditions consistent with the formation and survival of the Galilean satellites result for a wide range of gas-starved disks produced during the slow inflow of gas and solids into circumjovian orbit.

In the remainder of this section, we review some issues concerning late-stage Jovian accretion, modes of satellite formation, and relevant properties of the Galilean satellites. We discuss key disk processes in § 1.4.

1.1. *Growth of Jupiter*

In the core accretion model (e.g., Bodenheimer & Pollack 1986; Pollack et al. 1996; Bodenheimer, Hubickyj, & Lissauer 2000), a prolonged phase of solid and gas accretion gives way to the runaway accretion of gas once a protoplanet has achieved a critical core mass of $\sim 15\ M_\oplus$. During

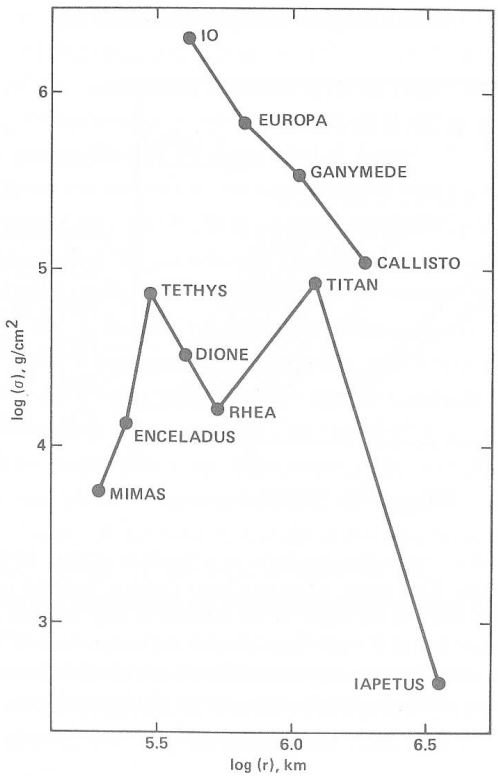

FIG. 1.—Minimum mass subnebulae for the Jupiter and Saturn satellite systems (from Pollack & Consolmagno 1984). The protosatellite disk surface density profile was constructed by spreading the mass of each satellite, augmented to match a solar proportion of elements, over an annulus centered on the current satellite orbit. Similarly dense disks have been utilized in previous models of Galilean satellite formation.

the runaway phase, a positive feedback exists as the rate of inflowing gas is regulated by the rate of contraction of the envelope, with the latter becoming increasingly rapid as the planet grows (Pollack et al. 1996). As long as gas accretion is unabated, the giant planet remains extended to its accretion radius, which for Jupiter's final growth stages is comparable to its Hill radius, $R_{\rm H} = a(M_p/3\ M_\odot)^{1/3}$, where a and M_p are the planet orbital radius and mass, respectively, and $M_\odot$ is the solar mass. Since $R_{\rm H}/R_{\rm J} \approx 744(M_p/M_{\rm J})^{1/3}$ (where $R_{\rm J} = 71,492$ km and $M_{\rm J} = 1.90 \times 10^{30}$ g $= 318\ M_\oplus$ are the current radius and mass of Jupiter), the planet in its expanded stage is vastly larger than the current Galilean system, for which $a/R_{\rm J} = 5.9 \rightarrow 26.4$ (Table 1).

The planet's radius shrinks relative to $R_{\rm H}$ when the rate of gas accretion can no longer keep up with that needed to compensate for the planet's increasing rate of contraction (e.g., Bodenheimer & Pollack 1986). A reasonable upper limit on the gas accretion rate is $\dot{M}_{\rm max} \sim 10^{-2}\ M_\odot\ {\rm yr}^{-1}$ (e.g., Hayashi, Nakazawa, & Nakagawa 1985; Bodenheimer & Pollack 1986; Bodenheimer et al. 2000). Calculations of the growth of Jupiter by Tajima & Nakagawa (1997) that did not impose any limit on the gas accretion rate found that for $M_p > 70\ M_\oplus$, an accretion rate in excess of $\dot{M}_{\rm max} \sim 10^{-2}\ M_\oplus\ {\rm yr}^{-1}$ would be required to maintain $R_p \approx R_{\rm H}$ (their Fig. 7). This suggests that in the later stages of its growth, Jupiter would likely not fill its entire Hill sphere (see also Pollack & Bodenheimer 1989). Recent models predict a full-mass Jupiter would require 10^6 yr to contract to $R_p \sim 1.9R_{\rm J}$, at which time it would have an effective temperature $\sim$800 K (e.g., Burrows et al. 1997, 2001); by 10^7 yr, $R_p \sim 1.5R_{\rm J}$ and $T_{\rm eff} \sim 500$ K (e.g., Hubbard, Burrows, & Lunine 2002). Thus, the Galilean satellites presumably formed late in Jupiter's growth.

Jupiter will likely have opened a gap in the protoplanetary disk prior to the completion of its growth; for typical assumed values of the solar nebular viscosity, gap opening (see § 2) is predicted for $M_p \geq O(10^2)\ M_\oplus$ (e.g., Bryden et al. 1999; Ward & Hahn 2000). However, recent hydrocode simulations in both two dimensions (e.g., Lubow, Siebert, & Artymowicz 1999; Bryden et al. 1999) and three dimensions (e.g., Kley, D'Angelo, & Henning 2001; D'Angelo, Henning, & Kley 2002; Lubow, Bate, & Ogilvie 2002) find continuing accretion onto Jupiter *after* gap opening, with $\dot{M} \sim 10^{-2}$ to $10^{-4}\ M_\oplus\ {\rm yr}^{-1}$ (or a Jovian mass in 10^4–10^6 yr), depending on the assumed nebular viscosity, disk surface density, and scale height. Actual gas accretion rates could be smaller if the nebula were dissipating (simulations typically assume a full minimum mass nebula), or if the solar nebula had a lower viscosity than can be adequately treated by hydrocode models.[1]

Simulations suggest that post–gap-formation gas flow within the Hill sphere (e.g., Fig. 2, from Lubow et al. 1999) involves streams of material entering near the L1 and L2 points, which then mutually collide to yield two shocked regions. A significant decrease in specific angular momentum of the shocked material then causes it to spiral inward toward the planet (Lubow et al. 1999; D'Angelo et al. 2002). Within $\sim 0.1R_{\rm H}$, there is evidence of a circumplanetary disk with a generally circular prograde flow.

1.2. *Satellite Formation Scenarios*

Several modes of formation have been proposed for the Galilean satellites (see, e.g., review by Pollack, Lunine, & Tittemore 1991). In the "spin-out disk" model, it is

[1] There is numerical viscosity associated with hydrocode simulations which generally limits modeled nebular disk viscosities to $\alpha > O(10^{-4})$ (e.g., see discussion in Bryden et al. 1999).

TABLE 1
PROPERTIES OF THE GALILEAN SATELLITES

Satellite	$a/R_{\rm J}$	M_S (10^{25} g)	R_S (km)	ρ_S (g cm^{-3})	$f_{\rm Si} = \dfrac{1-(\rho_{\rm ice}/\rho_S)}{1-(\rho_{\rm ice}/\rho_{\rm Si})}$
Io	5.9	8.93	1821	3.53	1
Europa	9.4	4.80	1561	3.01	0.85→1
Ganymede	15.0	14.8	2631	1.94	0.43→0.73
Callisto	26.4	10.8	2410	1.83	0.42→0.66

NOTE.—Silicate mass fractions from Schubert et al. 1986.

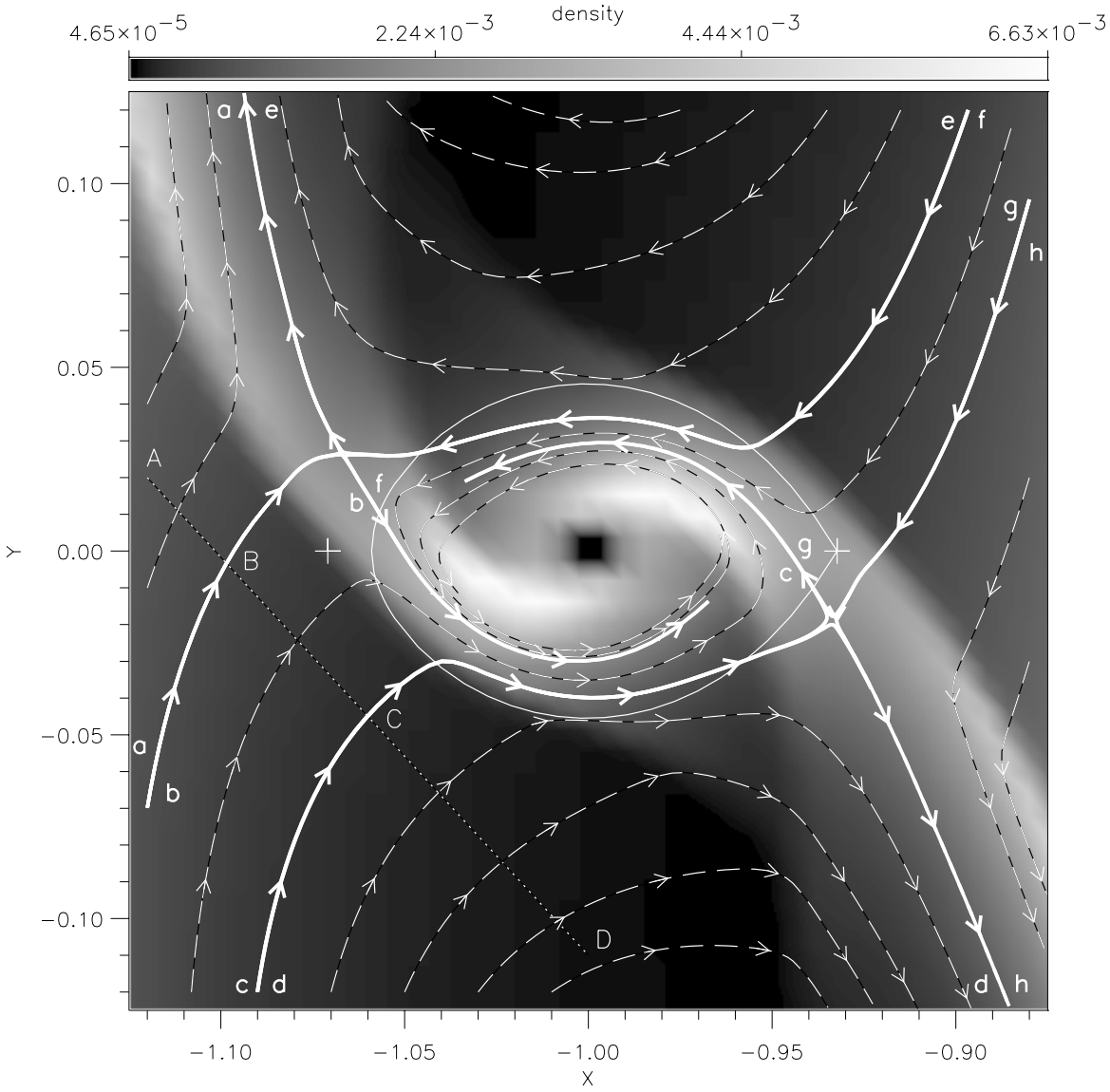

FIG. 2.—Density close-up of the Roche lobe of a Jovian mass planet located in a gap, shown in Cartesian coordinates scaled by the planet's orbital radius. Crosses indicate the L1 and L2 points; sample streamlines are shown by dashed lines (from Lubow et al. 1999, their Fig. 4).

assumed that the contraction of the planet to a scale smaller than the satellite system postdates nebular dispersal. As the planet contracts, outer layers of the envelope containing sufficient specific angular momentum to remain in bound orbit are "shed," forming a circumplanetary disk (Korycansky, Bodenheimer, & Pollack 1991). A requirement of this model is that sufficient rock and ice are contained in the outer envelope to account for the mass of solids in the satellites, perhaps accomplished through convective mixing within the planet (Bodenheimer & Pollack 1986).

The "accretion disk" model assumes that the contraction of the planet to a scale of less than a few R_J occurred prior to the complete removal of the solar nebula. Late-inflowing gas containing sufficient angular momentum for centrifugal force balance at an orbit of ~20–30 R_J (e.g., Ruskol 1982), then leads to the formation of a circumplanetary disk, similar to the situation depicted in Figure 2. A requirement for this model is that inflowing material contain a mixture of gas and solids, or that some fraction of local ice and rock still be contained in particles small enough to be carried inward with the gas. The model we advocate in § 3 is a variation on this theme.

Satellite formation from an "impact-generated disk" is the leading candidate for the formation of the Moon—and an intriguing possibility for Uranus—but the case for a late giant impact for Jupiter is weaker, given its extremely low obliquity. The "co-accretion" model involves the creation of orbiting material through collisions of planetesimals occurring within Jupiter's Hill sphere, and appears most consistent with the scale and orbital characteristics of the small irregular satellites.

1.3. *Galilean Satellite Constraints*

We infer from the very existence of the Galilean satellites that at least the last generation of large, similarly sized satellites formed in conditions that allowed for their survival

against orbital decay due to density wave interaction with their precursor gas disk (e.g., Ward 1997) and aerodynamic gas drag (e.g., Adachi, Hayashi, & Nakazawa 1976). The physical and orbital characteristics of the current satellites also provide key constraints (e.g., Table 1). The current orbital radii (in particular those of the inner three) have been altered from their primordial values as orbits expanded due to tidal interaction with Jupiter (e.g., Yoder & Peale 1981). Even after whatever tidal expansion they may have experienced in their history, the Galilean satellites are currently located in very central orbits compared to the Jovian Hill radius, with the outermost
having $a \sim 0.035 R_{\rm H}$.

The total mass in solids (ice + rock) in the current satellites is $\approx 4 \times 10^{26}$ g, or $\sim 2 \times 10^{-4} M_{\rm J}$. Assuming a solar gas-to-solids ratio $O(10^2)$ implies a required total mass to yield the satellites of 4×10^{28} g. The observed radial gradient in the satellites' bulk densities is associated with a decreasing silicate mass fraction, $f_{\rm Si}$, with distance. A silicate composition for Io, a hydrated silicate composition for Europa, and a Ganymede and Callisto that are roughly 50% rock and 50% ice are implied (e.g., Schubert, Spohn, & Reynolds 1986). The standard interpretation is that the protosatellite environment had a decreasing radial temperature profile, with sufficiently low temperatures exterior to the orbit of Ganymede to allow for significant incorporation of water ice (e.g., Lunine & Stevenson 1982).

The final constraint we consider is the apparent incomplete differentiation of Callisto. The most recent measurements (Anderson et al. 2001) of the moment of inertia of Callisto find $I/MR^2 \sim 0.3549 \pm 0.0042$, i.e., too small for a homogenous Callisto ($I/MR^2 \sim 0.4$), but too large for a completely differentiated object according to two- and three-layer interior models that assume hydrostatic equilibrium (Anderson et al. 2001).[2] At face value, these results imply that Callisto's formation did not involve the large-scale melting of ice. Accounting for only the release of gravitational binding energy during accretion, and assuming that energy is deposited and radiated away from the growing satellite's surface, an accretion time $\geq 10^5$ yr is required for a surface temperature rise $\Delta T \leq 270$ K in a Callisto-sized satellite (e.g., Stevenson, Harris, & Lunine 1986, Fig. 6; also B. Lane and D. Stevenson 2000, private communication). This is an extremely restrictive constraint, given that the orbital period at Callisto is only about 2 weeks. Predicted accretion times for Callisto assuming a minimum mass subnebula (see below) are $\leq 10^3$ yr; this time interval would imply $\Delta T \sim 1000$ K from release of binding energy alone.

In contrast, similarly sized and composed Ganymede appears highly differentiated, with $I/MR^2 = 0.3118 \pm 0.0005$ (W. B. Moore 2002, private communication) and an apparently molten core (Anderson et al. 1996). The surface of Ganymede also shows evidence of extensive resurfacing, which is absent on Callisto. From the standpoint of a satellite formation model, the apparent Ganymede-Callisto dichotomy reduces to three basic possibilities: (1) Callisto and Ganymede both formed rapidly, but conditions during accretion were such as to produce a differentiated Ganymede but only a partially differentiated Callisto. This possibility was evaluated by Lunine & Stevenson (1982) and Coradini et al. (1989) and generally found to be quite restrictive.[3] (2) Callisto's accretion interval was substantially prolonged relative to those of the other Galilean satellites (e.g., Mosquiera et al. 2001). (3) The accretion interval of all of the satellites was prolonged, with observed evidence of melting/heating on the inner three satellites influenced by subsequent heating due to tidal interactions, possibly higher silicate mass fractions,[4] and/or higher subnebula disk temperatures. We believe that the most successful and least restrictive disk models are consistent with scenario 3.

1.4. *Disk Processes*

We define a "minimum mass subnebula" (MMSN) disk to contain a mass in solids equal to the mass of the current satellites augmented to solar composition and spread out to 30 $R_{\rm J}$, with an average surface density of solids of $\sigma_s \approx 3 \times 10^3$ g cm^{-2} and an average gas surface density $\sigma_G \sim f \sigma_s \approx 3 \times 10^5$ g cm^{-2}, where $f_\odot \sim 10^2$ is the solar gas-to-solids ratio.

Orbital periods range from about 2 days at Io's orbit to about 2 weeks at Callisto's orbit, with correspondingly rapid collision times for orbiting material. The timescale for accretion of an object of radius R_S at orbital distance r (e.g., Lissauer & Stewart 1993; Ward 1996) is

$$\tau_A \approx \frac{1}{\Omega} \frac{\rho_S R_S}{\sigma_s F_g} \sim 50 \text{ yr} \left(\frac{R_S}{2500 \text{ km}} \right) \left(\frac{\rho_S}{2 \text{ g cm}^{-3}} \right) \left(\frac{10}{F_g} \right) \times \left(\frac{3 \times 10^3 \text{ g cm}^{-2}}{\sigma_s} \right) \left(\frac{r}{15 R_{\rm J}} \right)^{3/2}, \quad (1)$$

where Ω is orbital frequency, ρ_S is the bulk density of the object accreting, and $F_g \equiv 1 + (v_{\rm esc}/v_\infty)^2$ is the gravitational focusing factor for colliding objects with a relative velocity at infinity of v_∞ and a mutual escape velocity $v_{\rm esc}$. We stress that equation (1) is appropriate for a disk with an approximately constant total mass. Alternatively, if mass is delivered to the disk on a timescale that is long compared to equation (1), then the overall satellite accretion time will be regulated by the slower inflow rate, as discussed in § 3 (eq. [27]).

Accreting solids will interact with the gaseous component of the disk through both aerodynamic gas drag (e.g., Adachi et al. 1976) and gravitational torques (e.g., Ward 1993, 1997; Papaloizou & Larwood 2000). The orbital decay timescale of an object due to gas drag within a disk with sound

[2] The allowable amount of differentiation in Callisto has increased with recently improved measurements that imply decreased values for I/MR^2 over those obtained earlier. This has led to some skepticism in the undifferentiated Callisto interpretation (Peale 1999); others (McKinnon 1997) point out that nonhydrostatic effects could mimic the appearance of a partially differentiated satellite.

[3] For satellites with optically thick atmospheres, LS82 found that a preferred size range of infalling icy planetesimals would be subject to gas drag breakup and then aerodynamic breaking during their descent into a satellite's atmosphere. Icy fragments reaching the surface could then cool Callisto, which in combination with cooler circumjovian disk temperatures, could prevent Callisto from substantially melting while still predicting a fully melted Ganymede.

[4] The degree of postformation heating in a satellite can be affected by the silicate mass fraction, since the amount of long-lived radioactive isotopes is proportional to $f_{\rm Si}$ (Friedson & Stevenson 1983; Coradini et al. 1989).

speed c is

$$\tau_{\rm GD} \approx \frac{8}{3C_D}\frac{1}{\Omega}\left(\frac{\rho_S R_S}{\sigma_G}\right)\left(\frac{r\Omega}{c}\right)^3 \sim 10^3 \text{ yr}\left(\frac{10}{C_D}\right)\left(\frac{R_S}{2500 \text{ km}}\right)\left(\frac{\rho_S}{2 \text{ g cm}^{-3}}\right) \times \left(\frac{0.1}{c/r\Omega}\right)^3\left(\frac{3\times 10^5 \text{ g cm}^{-2}}{\sigma_G}\right)\left(\frac{r}{15R_{\rm J}}\right)^{3/2}, \quad (2)$$

where $C_D = C_1 + C_2[GM_S/(R_S c^2)]^2$ is the drag coefficient (e.g., Takeda et al. 1985; Ohtsuki, Nakagawa, & Nakazawa 1988), and C_1 and C_2 are constants of order unity. For a Galilean-sized satellite and $c \sim O(1)$ km s^{-1}, $C_D \sim O(10)$; for objects too small to gravitationally perturb the gas, $C_D \sim O(1)$.

A perhaps more important mode of interaction for large satellites is disk tidal torques (e.g., Ward 1993, 1997). A satellite excites density waves in a gas disk at Lindblad resonances, whose reaction torques on the satellite cause a net inward migration ("type I decay") with a timescale that is inversely proportional to the satellite's mass, M_S,

$$\tau_{\rm I} \approx \frac{1}{C_a\Omega}\left(\frac{M_{\rm J}}{M_S}\right)\left(\frac{M_{\rm J}}{r^2\sigma_G}\right)\left(\frac{c}{r\Omega}\right)^2 \sim 10^2 \text{ yr}\left(\frac{3}{C_a}\right)\left(\frac{2500 \text{ km}}{R_S}\right)^3\left(\frac{2 \text{ g cm}^{-2}}{\rho_S}\right) \times \left(\frac{c/r\Omega}{0.1}\right)^2\left(\frac{3\times 10^5 \text{ g cm}^{-2}}{\sigma_G}\right)\left(\frac{15R_{\rm J}}{r}\right)^{1/2}, \quad (3)$$

where C_a is a torque asymmetry parameter that is a function of the disk's radial surface density and temperature profiles (e.g., Goldreich & Tremaine 1980; Ward 1986, 1989, 1997; Artymowicz 1993; Tanaka, Takeuchi, & Ward 2002). The ratio of a satellite's lifetime against type I decay versus gas drag is independent of σ_G,

$$\frac{\tau_{\rm I}}{\tau_{\rm GD}} \sim 0.1\left(\frac{C_D}{10}\right)\left(\frac{3}{C_a}\right)\left(\frac{2500 \text{ km}}{R_S}\right)^4 \times \left(\frac{2 \text{ g cm}^{-3}}{\rho_S}\right)^2\left(\frac{c/r\Omega}{0.1}\right)^5\left(\frac{15R_{\rm J}}{r}\right)^2, \quad (4)$$

implying that the most rapid loss mechanism for the final stages of satellite growth may well be disk torques rather than aerodynamic gas drag.

Type I inward migration would transition to the typically slower type II decay if a satellite became large enough to open a gap in the disk. One criterion for gap opening (e.g., Lin & Papaloizou 1986; Ward 1986) is that the cumulative torque on the disk by the satellite must exceed the rate of angular momentum transfer due to the disk's viscosity. Adopting an "alpha model" for the disk viscosity (Shakura & Sunyaev 1973), $\nu \equiv \alpha c H = \alpha c^2/\Omega$ (where $H \approx c/\Omega$ is the disk scale height), the gap opening criterion assuming local wave damping is (e.g., Ward & Hahn 2000)

$$\frac{M_S}{M_{\rm J}} > c_\nu\sqrt{\alpha}\left(\frac{c}{r\Omega}\right)^{5/2} \sim 10^{-4}c_\nu\left(\frac{\alpha}{10^{-3}}\right)^{1/2}\left(\frac{c/r\Omega}{0.1}\right)^{5/2}, \quad (5)$$

where c_ν is $O(1$–$10)$, and typical α values range from 0.1 for a highly turbulent disk to 10^{-4} (e.g., Cabot et al. 1987). The mass cutoff in equation (5) is just larger than the mass of Ganymede for $c_\nu = 1$ and $\alpha = 10^{-3}$. In the limit of an inviscid disk, the gap opening criterion asymptotes to an inertial one based upon a comparison between the gap opening time and the time for a satellite to migrate across a distance equal to the gap width due to type I decay (Hourigan & Ward 1984; Ward & Hourigan 1989; Ward 1997). This gap opening criterion is

$$\frac{M_S}{M_{\rm J}} > \left(\frac{\pi\sigma_G r^2}{M_{\rm J}}\right)\left(\frac{c}{r\Omega}\right)^3 \sim 2\times 10^{-5}\left(\frac{M_d/M_{\rm J}}{0.02}\right)\left(\frac{c/r\Omega}{0.1}\right)^3. \quad (6)$$

If a satellite opens a gap, it will still generally experience an inward migration that is controlled by the viscous spreading of the disk (type II decay), with a timescale

$$\tau_{\rm II} \approx \tau_\nu = \frac{r_d^2}{\nu} \approx 10^3 \text{ yr}\left(\frac{10^{-3}}{\alpha}\right)\left(\frac{r_d}{30R_{\rm J}}\right)^{3/2}\left(\frac{0.1}{c/r\Omega}\right)^2, \quad (7)$$

where r_d is the disk outer radius.

The Kelvin-Helmholtz cooling time for the MMSN disk assuming the only energy source is the internal heat of the disk is (e.g., Lunine & Stevenson 1982)

$$\tau_{\rm KH} \approx \frac{C\sigma_G T_c}{2\sigma_{\rm SB}T_d^4} \sim O(10^3) \text{ yr}\left(\frac{250}{T_c}\right)^3\tau, \quad (8)$$

where $\sigma_{\rm SB} = 5.67\times 10^{-5}$ erg cm^{-2} s^{-1} K^{-4} is the Stephan-Boltzman constant, C is specific heat, T_c and T_d are the midplane and effective photospheric disk temperatures, respectively, and τ is the vertical gas optical depth, $\tau \equiv \sigma_G K$, where K is the disk opacity in cm^2 g^{-1}. From the equations of thermal and radiative equilibrium (e.g., Schwartzchild 1958; see also Lunine & Stevenson 1982), for a constant K with height the midplane temperature is approximately related to the effective temperature through

$$T_c \cong \left\{1 + \frac{3}{2}\left[1 - \left(\frac{T_{\rm neb}}{T_d}\right)^4\right]\tau\right\}^{1/4} T_d, \quad (9)$$

where $T_{\rm neb}$ is the ambient nebular temperature, likely $\sim$100–150 K near Jupiter (e.g., Lewis 1974).

Relevant disk energy sources include luminosity from Jupiter and viscous dissipation. For a radially optically thick disk in vertical hydrostatic equilibrium with scale height, $H = c/\Omega$, Jupiter's luminosity will provide energy to an annulus in the disk extending from r to $(r + \Delta r)$ at a rate

$$\dot{E}_J \approx 2\sigma_{\rm SB}T_{\rm J}^4\left(\frac{R_{\rm J}}{r}\right)^2 2\pi r[H(r+\Delta r) - H(r)] \approx \frac{9}{4}\sigma_{\rm SB}T_{\rm J}^4\left(\frac{R_{\rm J}}{r}\right)^2\left(\frac{c}{r\Omega}\right)2\pi r\Delta r, \quad (10)$$

where $T_{\rm J}$ is Jupiter's temperature, and we have assumed a $T_c \propto 1/r^{3/4}$ dependence. Viscous dissipation and energy loss due to radiative cooling within an annulus yield

$$\dot{E}_\nu = \tfrac{9}{4}\nu\Omega^2\sigma_G 2\pi r\Delta r, \qquad \dot{E}_{\rm rad} = -2\sigma_{\rm SB}(T_d^4 - T_{\rm neb}^4)2\pi r\Delta r. \quad (11)$$

2. SATELLITE FORMATION FROM A GAS-RICH MMSN DISK

A straightforward approach to satellite formation is to assume that a protosatellite disk containing all of the mass necessary to form the satellites was created on a timescale that is short compared to the disk evolution timescale—i.e., the minimum mass subnebula model described above. In this section, we discuss a number of problems with this approach that have led us to abandon it in favor of the starved disk model presented in the next section. Readers wishing to advance directly to this new model can skip to § 3 without loss of continuity.

2.1. *Previous Work*

The best candidate mechanism for producing an MMSN disk is the spin-out model. Another alternative would be forming a $\sim 0.02 M_{\rm J}$ disk during a final stage of gas inflow to Jupiter (e.g., Coradini et al. 1989; Makalkin, Dorofeeva, & Ruskol 1999), also discussed below.

Korycansky et al. (1991) modeled the growth of a Saturnian-mass planet, using a one-dimensional model including rotation. They found that as gas accretion ceased, the planet rapidly contracted and shed its outer layers to form a disk containing roughly 1% of the primary's mass between about 25 and 400 planetary radii.[5] Depending on the composition of the outer envelope layers, the resulting disk gas-to-solid ratio, f, could be similar to solar composition or even higher (e.g., Pollack et al. 1991).

These results suggest the deposition of spin-out material occurs well outside the region of the regular satellites on a timescale of only $\sim 10^2$ yr. However, unless gas accretion was terminated on a similarly short timescale, this contraction would actually be accompanied by additional gas inflow, which could affect the spin-out and disk deposition process. The dynamics of the creation of a Jovian spin-out disk might also differ from that of a Saturnian-mass planet, given the planet's higher mass (and thus faster initial contraction rate in the absence of accretion; Pollack & Bodenheimer 1989), and that Jupiter may not have completely filled its Hill sphere during all of its gas accretion phase. Given such uncertainties—the resolution of which would be of great interest but is beyond the scope of the work here—we consider a spin-out–produced MMSN disk as defined above.

The most comprehensive model of Galilean satellite formation in an MMSN-style disk is the work of Lunine & Stevenson (1982, hereafter LS82). They considered a static disk, with no mass inflow or viscous radial transport, the justification being that the timescale for satellite accretion (eq. [1]) is much shorter than that of the cooling time of the disk (eq. [8]). Several difficulties were revealed by their investigation. The disk profile in LS82 was constructed by setting the disk temperature at Ganymede's orbit to allow for the condensation of ice. However (as the authors point out), for the high MMSN gas surface density, such a low temperature could be achieved only for a practically inviscid disk. Ignoring any possible contribution from Jupiter's luminosity, an upper limit on the disk viscosity that allows for potential ice stability near Ganymede's orbit can be established by balancing viscous dissipation (eq. [10]) with radiation from the disk surface (eq. [11]). Assuming a low, solely gaseous disk opacity with, e.g., $K = 10^{-4}$ cm^2 g^{-1} gives $\tau \sim O(10)$ and $T_c \sim 2T_d$; for an ambient nebular temperature $T_{\rm neb} = 150$ K, $\alpha \leq O(10^{-6})$ is then required for even the photospheric temperature $T_d(15R_{\rm J}) \leq 230$ K. Thus, forming ice-rich Ganymede and Callisto necessitates a very low viscosity compared to typical values associated with circumstellar disks, e.g., $\alpha \sim 10^{-4}$–10^{-2} (e.g., Stone et al. 2000). Given that $\tau_A \ll \tau_{\rm KH}$ for an optically thick disk, it could be difficult to delay satellite accretion until the appropriately cold and viscously quiescent disk conditions were achieved to produce icy satellites. Instead, a first generation of rock-rich satellites might result. The satellite lifetimes against type I radial decay discussed in § 1 (and indeed cautioned about in LS82) would be exceedingly short in such a massive gas disk (eq. [3]). Thus, it is not obvious how a system of rocky satellites could be retained long enough for ice condensation to ensue.

In the LS82 study, Ganymede and Callisto form on similarly short timescales and with optically thick atmospheres. Estimates of their resulting surface temperatures suggested that both satellites would have undergone significant differentiation. If a protracted accretion of $\geq 10^5$ yr is required to account for Callisto's incomplete differentiation, this constraint would not be satisfied in a MMSN, in which the satellite accretion times would be short and similar (eq. [1]).[6]

An important advance was made by Coradini et al. (1989; see also Coradini & Magni 1984 for the Saturnian satellite system), who incorporated viscous evolution of an accretion disk formed via nebula mass inflow into circumjovian orbit. With a methodology similar to that which we adopt in § 3, they computed the steady-state disk conditions using the Lynden-Bell & Pringle (1974) formalism. The disk was conceived to be highly convective with a strong turbulence viscosity parameter $\alpha \sim 10^{-1}$ in the inner satellite region. A starting assumption was that the steady-state mass of gas and solids in the disk should equal the augmented mass of the current satellites. This constrained the rate of mass infall to $\dot{M} \sim 10^{-1}\ M_\oplus\ {\rm yr}^{-1}$, corresponding to $\tau_{\rm J} = M_{\rm J}/\dot{M}_{\rm J} \sim 10^3$ yr.

The midplane temperatures predicted by the Coradini et al. models were $>10^3$ K inside $30R_{\rm J}$ (e.g., Coradini et al. 1989, their Fig. 18). A two-part scenario was thus proposed whose first stage involved the creation of a hot, highly convective accretion disk during the rapid mass infall to Jupiter, while the second phase would occur after inflow stopped, during which time disk cooling allowed for ices and hydrated silicates to condense and the disk to become quiescent. During the initial phase, solid accretion would be precluded by high temperatures or viscous turbulence in the disk, whereas in the latter, satellite accretion would proceed along the lines of the LS82 model, i.e., in the absence of gas inflow. The assumption that satellite accretion would occur after mass inflow to Jupiter has ceased would require that

[5] This process provides one means of removing sufficient angular momentum from the planet to reduce its rotation rate to something comparable to that of the current gas giants, although there may be others (e.g., Takata & Stevenson 1996; Quillen & Trilling 1998).

[6] We note that if special circumstances are invoked to prolong the accretion time of just Callisto (Mosquiera et al. 2001 LPSC), then the inner three more rapidly forming satellites would still be subject to loss as discussed below in § 2.2—due to either type I or II decay or gas drag—so long as their precursor gas disk persists.

the inflow cut off extremely rapidly, specifically on a timescale that is short compared to disk evolution processes. The initially hot and convective disk considered in Coradini et al. would viscously spread on a timescale of only $\tau_\nu \sim r_d^2/\nu$, or $O(10)$ yr for the assumed values $r_d = 10^2 R_J$ and $\nu \sim 10^{15}$ cm^2 s^{-1}, a timescale much shorter than τ_{KH} from equation (8). Thus, it seems likely that much of the disk mass would viscously evolve onto the central object before temperatures cooled enough to allow for ices to condense.

Makalkin et al. (1999) considered an accretion disk model with a much slower inflow rate $\dot{M} \sim 10^{-6}\ M_\oplus$ yr^{-1}, or $\tau_J = M_J/\dot{M}_J \sim 10^8$ yr. They emphasized the impossibility of simultaneously satisfying the temperature and total mass requirements for the Galilean satellites. Two possible alternative disk models were suggested: a highly inviscid MMSN disk which satisfied the total mass requirement (similar to that which we consider in this section), or a low-mass, viscous and appropriately low-temperature disk (similar to that considered in the next section). Makalkin et al. (1999) concluded that it is uncertain which disk model is more promising. In this section and the next, we extend this and earlier works by considering a wide range of inflow rates and possible disk viscosities, as well as the effects of satellite-disk interactions; the latter provide substantial additional constraints, as we discuss next for the case of the MMSN disk.

2.2. *Satellite Survival*

It was argued in § 1.4 that both accretion and type I decay timescales are extremely short in a MMSN disk with

$$\frac{\tau_A}{\tau_I} \approx 0.5\left(\frac{C_a}{3}\right)\left(\frac{R_S}{2500\text{ km}}\right)^4\left(\frac{\rho_S}{2\text{ gm cm}^{-3}}\right)^2 \times \left(\frac{0.1}{c/r\Omega}\right)^2\left(\frac{10}{F_g}\right)\left(\frac{f}{100}\right)\left(\frac{r}{15R_J}\right)^2. \quad (12)$$

Given the closeness of this ratio to unity, explaining how a Galilean-sized satellite could accrete without being lost to the primary is a key issue. Since $\tau_A/\tau_I \propto f$, one way to increase the likelihood of satellite survival is to decrease the effective f in the accreting region. A disk composed at the outset of material with $f \ll f_\odot$ would alleviate this situation, but a primary concern that has been raised with the spin-out model is whether it would be able to provide even a solar proportion of solids, given that solids in the planet will have likely been primarily concentrated in the core and would need to be well mixed in the outer envelope to be present in the spin-out disk at all (e.g., Pollack et al. 1991). Similar concerns exist for material inflowing from the solar nebula after its partial depletion of solids by the formation of the giant planet cores. Alternatively, one could postulate that the gaseous portion of the disk viscously spreads during accretion. Recall, however, the temperature argument above, which implies that a nearly inviscid disk is needed, so that $\tau_\nu \gg \tau_A, \tau_I$.

Assuming large satellites were able to accrete, they must continue to survive for the lifetime of their precursor disk. Here the relevant timescale comparison is

$$\frac{\tau_I}{\tau_\nu} \sim \frac{1}{C_a\Omega}\left(\frac{M_J}{M_S}\right)\left(\frac{M_J}{r^2\sigma_G}\right)\left(\frac{\nu}{r_d^2}\right)\left(\frac{c}{r\Omega}\right)^2 \sim O(10^{-4})\left(\frac{\alpha}{10^{-6}}\right) \quad (13)$$

for the values given in equations (3) and (7), so that the satellites are lost inward on timescales much shorter than that needed to viscously remove the disk for a cool, nearly inviscid disk.

So far, the above expressions assume full-strength type I torques. Could such torques and the resulting migration have been mitigated by wave reflection from disk boundaries (e.g., Ward & Canup 2002; Tanaka et al. 2002)? If waves reflect off the outer and inner disk edge, they can return a portion of their angular momentum flux to the resonance site. A standing wave pattern then develops on each side of the satellite as a result of the superposition of outgoing and incoming wave trains. In the case of total reflection, the returning wave modifies the launch conditions so that outgoing and incoming waves are symmetrical about the primary/secondary line and the net torque of the satellite vanishes. However, total reflection can occur only if the waves do not dissipate during their entire round trip; if they suffer significant dissipation, little torque reduction will occur.

From the dispersion relationship for density waves, the wavenumber $k \sim (D/c^2)^{1/2}$, where $D \equiv m^2(\Omega_S - \Omega)^2 - \kappa^2$ is the frequency distance from resonance, where $D = 0$ and κ is the epicyclic frequency (e.g., Goldreich & Tremaine 1979). The wavenumber increases as the waves propagate radially, causing them to wrap up in the familiar spiral pattern with m number of spiral arms. Far external to the resonance, $D \to m^2\Omega_S^2$ and $k \to m\Omega_S/c$; the most important resonances have wavenumbers of the order of $m \sim r\Omega_S/c$, for which k approaches r/H^2 and the wavelength is only a few percent of the scale height $H = c/\Omega$. On the other hand, the surface density at the outer edge of the disk cannot fall off more sharply than a scale height, since steeper gradients would be Rayleigh unstable (e.g., Lin et al. 2000; see also Agnor & Ward 2002). Consequently, should the outbound waves make it as far as the MMSN disk outer edge, they would penetrate this wing of the disk and shock dissipate. On the inward side of the satellite, some wave reflection may be possible if the inner disk extends to the planet, but this would exacerbate the tendency for satellite loss by reducing the outward torque on the satellite.

Even if the type I torques were somehow mitigated, satellites in a MMSN disk would still be vulnerable to orbital decay via aerodynamic drag. As noted by Lunine & Stevenson (1982), the gas drag timescale for the satellites is quite short in such a disk, $\sim O(10^3)$ yr (eq. [2]); thus, they could be lost on times comparable to or shorter than that needed to viscously remove the disk for $\alpha \leq 10^{-3}$.

From equation (6), Galilean-sized satellites could potentially open gaps in a low-viscosity disk, reducing the effectiveness of aerodynamic drag and causing a transition to type II decay. However, since the type II decay timescale is essentially the disk's viscous lifetime, satellites would still be lost as long as the disk is removed by diffusion. This fate could be avoided if the disk were removed by some nonviscous process on a timescale shorter than $\tau_\nu \approx O(\alpha^{-1})$ yr. Photoevaporation is sometimes invoked as a nonviscous disk removal mechanism, although the timescale for this is so long ($\sim 10^7$ yr, e.g., Hollenbach, Yorke, & Johnstone 2000) that the disk must be even more inviscid than our previous estimate with $\alpha < 10^{-7}$. Survival of the Galilean satellites via gap opening and transitioning to type II decay would then require that (1) the disk was extremely inviscid

and long-lived, (2) all four satellites were able to open gaps, and (3) the protosatellite disk is eventually removed via photoevaporation.

One inconsistency in this picture is the requirement of such a low disk viscosity. The interaction of the satellites themselves with the disk provides a source of angular momentum transport (e.g., Goodman & Rafikov 2001). In this regard, one must remain cognizant that gap opening does not actually shut off disk torques, but merely provides a mechanism whereby a satellite can seek a quasi-equilibrium where the inner positive and outer negative torques balance. Angular momentum continues to flow outward across the satellite's orbit, and this transport can be characterized as an effective viscosity. For instance, setting the time, $t_{\Delta L} \sim \Delta L/\Gamma$, necessary to remove all of the angular momentum, $\Delta L \approx O(\pi\sigma_G r^4\Omega)$, from the interior portion of the disk by the one-sided disk torque, $\Gamma \approx \mu_S^2\sigma_G r^2(r\Omega)^2(r/w)^3$, equal to an equivalent diffusion timescale $\sim r^2/\nu_{\rm eff}$, allows one to estimate an effective $\alpha_{\rm eff} \sim O[\mu_S^2(r/H)^3(H/w)^3] \approx 10^{-3}(H/w)^3$, where w is the gap half-width, H is the disk scale height, and $\mu_S \equiv M_S/M_{\rm J}$. For $w \sim H$, $\alpha_{\rm eff}$ is orders of magnitude larger than that necessary to allow for a photodissociative removal of the circumplanetary disk.

An extreme case would be to assume that a Galilean-sized satellite could open a very broad gap, so that disk material was shepherded out beyond the 2 : 1 and 1 : 2 resonances (although this may not be possible given the close spacing of the satellites). This would act to reduce both Γ and $\alpha_{\rm eff}$, with $(H/w)^3 \sim$ a few $\times 10^{-3}$ and $\alpha_{\rm eff} \sim 10^{-6}$. The zero-order disk torques would then be largely shut off, but the more distant first-order resonances (i.e., the 3 : 1 and 1 : 3) would still remain in the disk. These are $m = 2$ Lindblad resonances with pattern speeds of $\Omega_{\rm ps} \sim 3\Omega_S/2$, $\Omega_S/2$, respectively; both act to excite the satellite's eccentricity (Goldreich & Tremaine 1980; Goldreich & Sari 2002). Concentrating on the inner Lindblad resonance (ILR) as an example, the first-order torque is (e.g., Ward & Hahn 2000; Ward & Canup 2000)

$$\Gamma_1 \sim \frac{\pi^2}{6} e^2\mu_S^2(\sigma_G r^2)(r\Omega_S)^2\left(\frac{\Omega_S}{\Omega_{\rm res}}\right)^2 \times \left(\gamma^2\frac{d^2b_{1/2}^{(2)}}{d\gamma^2} + 10\gamma\frac{db_{1/2}^{(2)}}{d\gamma} + 20b_{1/2}^{(2)}\right)^2 \approx O(10)\, e^2\mu_S^2(\sigma_G r^2)(r\Omega_S)^2 , \quad (14)$$

where the bracketed quantity is evaluated at the 3 : 1 resonance, $\gamma = r_{\rm res}/r = 1/3^{2/3} = 0.481$. The satellite eccentricity would then be excited at the rate[7]

$$\frac{1}{e}\frac{de}{dt} \approx \frac{-\Gamma_1\sqrt{1-e^2}}{M_S e^2 r^2\Omega_S}\left(1 - \frac{\Omega_{\rm ps}}{\Omega_S}\sqrt{1-e^2}\right) \approx 3\mu_S\mu_d\Omega_S , \quad (15)$$

where $\mu_d \equiv M_d/M_{\rm J}$. For $r = 15R_{\rm J}$, this corresponds to a characteristic e-growth time of only $\sim O(10^3)$ yr. To shut off this torque, the satellite would have to further shepherd the disk material $\Delta M_d \equiv 2\pi\sigma_G r^2(1-\gamma)$ beyond the 3 : 1, i.e., an additional distance $\delta r/r = 2^{-2/3}$ to $3^{-2/3} = 0.15$, but would have only the first-order torque Γ_1 available to do this. This requires $\int\Gamma_1 dt = \Delta L \sim \Delta M_d r^2\Omega(\delta r/2r) \approx$ a few $\times 10^{-2}\mu_d M_{\rm J} r^2\Omega_S$ more angular momentum be removed from the inner disk. Combining this with the eccentricity equation then implies a total e-growth during a hypothetical wide-gap phase of $\Delta e^2 \sim$ a few $\times\, 10^{-2}(\mu_d/\mu_S) \sim O(1)$. At large eccentricities, other higher order resonances would become important as well. Thus, even assuming a highly inviscid disk and the formation of very broad gaps around the satellites, it is dubious that the Galilean satellites could have occupied a MMSN disk for $\sim 10^7$ yr (i.e., $\sim 10^4$ e-folding times) without developing instabilities due to forced eccentricity growth.

2.3. *Jovian Obliquity*

We close this discussion by mentioning some completely independent evidence against a long-lived $\sim 10^7$ yr disk based on Jupiter's small $\sim 3^\circ$ obliquity. The current spin axis precession period of Jupiter is $\sim 4.5 \times 10^5$ yr, due mostly to the solar torque exerted on the Galilean satellites (e.g., Ward 1975; Harris & Ward 1982; Tremaine 1991). However, this would have been up to $\sim O(10^2)$ shorter if a MMSN were present. If this disk were subsequently photoevaporated after the solar nebula itself was dissipated, Jupiter's precession frequency would have drifted through one of the mutual orbital precession frequencies of Jupiter and Saturn, i.e., the so-called ν_{16} that describes the precession of their orbital nodes with a period of $P_{16} \sim 5 \times 10^4$ yr. An adiabatic passage could generate an obliquity of (Henrard & Murigande 1987; Ward & Hamilton 2002)

$$\cos\theta = \frac{2}{(1+\tan^{2/3} I)^{3/2}} - 1 , \quad (16)$$

where $I \sim 0.^\circ 36$ is the amplitude of Saturn's perturbation of the Jovian orbital inclination (e.g., Applegate et al. 1986). This gives a limiting obliquity of $\theta = 25.^\circ 6$. If passage is fast enough to be nonadiabatic, the final obliquity is rate dependent, i.e.,

$$\theta \approx \frac{2\pi I}{P_{16}}\left(\frac{2\pi}{\dot\alpha_s}\right)^{1/2} \quad (17)$$

(Ward, Columbo, & Franklin 1976), where α_s denotes the spin axis precession parameter, which is a function of the circumplanetary disk and satellite masses in addition to the Jovian oblateness (e.g., Ward 1975). We define $\tau_{\rm pole} \equiv \alpha_s/\dot\alpha_s$ and calculate its value when equation (17) is comparable to Jupiter's current obliquity, viz., $\tau_{\rm pole} \sim P_{16}(\theta/2\pi I)^2 \approx O(10^5)$ yr. But since the change in α_s would be due primarily to dissipation of the protosatellite disk, we conclude that a disk life much longer than this is not consistent with Jupiter's low-obliquity spin state.

Thus, multiple difficulties emerge from the standard "minimum mass subnebula" model, and a single, self-consistent scenario does not simultaneously satisfy the system constraints. The simplest means of removing these difficulties would be to have the final stages of satellite formation occur in an environment that was enhanced in solids relative to the solar gas-to-solids ratio. By reducing f, the lifetimes of the satellites against various processes associated with the gas disk are increased; in addition, a lower

[7] The innermost corotation resonance that would damp e would be inside the gap.

mass gas disk eases the constraints on the disk's viscosity needed to yield sufficiently low temperatures.

3. SATELLITE FORMATION FROM A GAS-STARVED ACCRETION DISK

Given the extremely rapid circumplanetary disk process timescales, it is difficult to imagine that satellite accretion could "wait" until gas inflow to Jupiter had completely stopped. Instead, we consider it more reasonable that gas accretion onto Jupiter ended on a timescale that is long compared to relevant timescales in a circumjovian disk, so that satellite growth occurred in the presence of the final gas inflow. Assuming that the cutoff in gas accretion was sufficiently prolonged that Jupiter had time to contract to a scale smaller than the current satellite orbits, the gas inflow rates during satellite accretion would presumably be lower than the peak rates experienced during Jovian runaway gas accretion; otherwise, the planet would have likely still been quite distended. The creation of a circumplanetary accretion disk during such a slow-inflow period would yield a less massive steady-state disk than the MMSN considered above and by earlier works. Here we explore this alternative gas-starved disk model.

3.1. *Origin of an Accretion Disk*

Recent hydrocode simulations describing planet-nebula interactions in the waning stages of Jupiter's growth reveal dynamical behavior within its Hill sphere and approaching the region of the regular satellites. Lubow et al. (1999) used two-dimensional simulations in which the planet's orbit was fixed to consider the behavior of a Jovian mass planet embedded in a disk with an assumed viscosity parameter of $\alpha = 4 \times 10^{-3}$. The pattern of flow shown in Figure 2 is similar to that obtained by recent three-dimensional simulations by D'Angelo et al. (2002) that additionally consider the back reaction of the perturbed disk on the planet. Flow into the Hill sphere enters through the L1 and L2 Lagrange points via two streams of material. After traveling about halfway around the Hill sphere, the streams mutually collide, producing a shocked region at a distance from the planet of about 100–200 R_J. The shocked material then flows toward the planet, forming a more quiescent prograde interior disk. D'Angelo et al. (2002) find a high-density "core" surrounding the central planet's position with an orbital radius $\sim 0.04 R_H \sim 30 R_J$ for a Jovian mass planet (their Fig. 17).

Unfortunately, with current resolutions the inner satellite region is typically described by only a few numerical "cells." Mass is removed from the innermost region in the course of a simulation to mimic accretion onto the planet at some assumed rate, which could influence inner disk surface densities. The hydrocode simulations do not self-consistently calculate the size of the central planet;[8] it is thus not clear what physical planet radius would be appropriate for the implied mass accretion rates, and the question of the relative timing of planetary contraction versus nebular dispersal remains an open and important one.

Below we formulate a generic disk model motivated by the overall properties of the above results, in which several key (but uncertain) quantities are treated as free parameters.

3.2. *Gas Disk Model*

Consider a circumjovian accretion disk (see Fig. 3) supplied by an inflow of material with some characteristic maximum specific angular momentum, j (e.g., Cassen & Summers 1983; Coradini et al. 1989). Inflowing material, containing some mass ratio f of gas-to-solids, is assumed for simplicity to be deposited into centrifugally supported orbits with a uniform flux per area, F_{in}, in the region extending to the radial distance $r_c \equiv j^2 G M_J$. The total rate of mass inflow is $F_* = \pi F_{in} r_c^2$. The disk is assumed to have some outer edge, r_d, at which disk material is stripped from the disk, perhaps by solar torques or through collision with the highly shocked regions that appear to be associated with mass flow into the Hill sphere. The steady-state gas surface density is then (Lynden-Bell & Pringle 1974; see Appendix)

$$\sigma_G(r) \approx \frac{4F_*}{15\pi\nu} \begin{cases} \frac{5}{4} - \sqrt{\frac{r_c}{r_d}} - \frac{1}{4}\left(\frac{r}{r_c}\right)^2 & \text{for } r < r_c \,, \\ \sqrt{\frac{r_c}{r}} - \sqrt{\frac{r_c}{r_d}} & \text{for } r \geq r_c \,, \end{cases} \tag{18}$$

where again the disk viscosity is $\nu \equiv \alpha c H = \alpha c^2/\Omega$, and c is the midplane sound speed.

A simple model estimates disk temperature by considering a balance between energy produced from mass infall, viscous dissipation, heating due to Jupiter's luminosity, and radiative cooling from the disk surface (eqs. [10] and [11]; e.g., Coradini et al. 1989; Makalkin et al. 1999). With the effective and midplane sound speeds given by $c_d^2(r) \equiv \mathscr{R} T_d(r)/\mu_{mol}$ and $c^2(r) \equiv \mathscr{R} T_c(r)/\mu_{mol}$, where $\mathscr{R} = 8.31 \times 10^7$ ergs molecule^{-1} K^{-1} is the gas constant, and μ_{mol} is the molecular weight in g molecule^{-1}, with $\mu_{mol} = 2$ for molecular hydrogen, the energy balance at an orbital radius r is

$$\frac{9}{4}\left[\sigma_{SB} T_J^4 \left(\frac{R_J}{r}\right)^2 \frac{c}{r\Omega} + \chi \alpha c^2 \Omega \sigma_G\right] = 2\sigma_{SB}\left[\left(\frac{2c_d^2}{\mathscr{R}}\right)^4 - T_{neb}^4\right] , \tag{19}$$

where $\chi \equiv 1 + \frac{3}{2}[r_c/r - \frac{1}{5}]^{-1}$, with the second term arising from the mass infall. At each disk radius, extending from

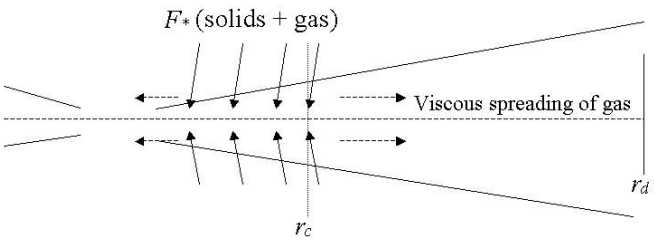

FIG. 3.—Schematic of accretion disk model described in § 3. Solids and gas are assumed to be delivered to circumplanetary orbit with some characteristic specific angular momentum such that they achieve orbit about the planet in a region extending from the surface of the planet out to some distance, r_c. Once in orbit, solids rapidly accumulate into objects large enough to decouple from the gas, while the gas component of the disk spreads viscously both onto the planet, and out to some assumed outer edge, r_d.

[8] An exception are recent simulations by A. Coradini presented at the 2002 June Eurojove conference in Lisbon, Portugal.

TABLE 2
NOMINAL DISK MODEL

T_J	500 K
r_c	$30R_J$
r_d	$150R_J$
f	100

the surface of the planet to outer edge r_d, we use an iterative method to determine $T_d(r)$, $T_c(r)$, $\nu(r)$, and $\sigma_G(r)$ self-consistently. Given an input value for α, F_*, and K, an initial guess for $\sigma_G(r)$ is used to calculate $T_c(r)$ from equation (18). These values, together with $c = c_d\{1 + 3\tau/2[1 - (T_{\rm neb}/T_d)^4]\}^{1/8}$, are then used to recalculate $\sigma_G(r)$ from equation (19), and the process is repeated until convergence is achieved.

Table 2 contains our nominal disk parameters. The relevant disk opacity is quite uncertain. For a dust-free disk, the mean Rosseland gaseous opacity is $K \sim 10^{-4}$ cm^2 g^{-1} (e.g., LS82; Ikoma, Nakazawa, & Emori 2000) for $T \sim 200$ K and a density $\rho_G \sim 10^{-5}$ g cm^{-3} (Mizuno 1980; cf. Stevenson et al. 1986), while absorption by micron and submicron sized grains could provide opacities as high as $K \sim 10^{-1}$ to 1 cm^2 g^{-1} for relevant disk temperatures (e.g., Bodenheimer et al. 1980; Chiang et al. 2001). Given this, we consider cases with $K = 10^{-4}$, 10^{-2}, and 1 to bracket a range of plausible conditions.

3.3. *Disk Temperature Profile*

The inflow rate is constrained by the requirement that temperatures be low enough for ice in the general region near Ganymede and Callisto's orbits. Assuming that viscous dissipation is the dominant energy source (as it is in the regular satellite region for all of the cases considered here), and $T_d^4 \gg T_{\rm neb}^4$,

$$T_d^4 \approx \frac{9\Omega^2}{8\sigma_{\rm SB}}\nu\sigma_G = \frac{3\Omega^2 F_*}{8\pi\sigma_{\rm SB}}\left[1 - \frac{4}{5}\sqrt{\frac{r_c}{r_d}} - \frac{1}{5}\left(\frac{r}{r_c}\right)^2\right] \quad (20)$$

for $r < r_c$, and $T_d \propto 1/r^{3/4}$ approximately. *The effective disk temperature is a function of the rate of inflow, F_*, but independent of both the gas surface density and the disk viscosity*. Thus, for optically thin disks, F_* and the disk scale parameters (r_c and r_d) determine the disk temperature profile. For optically thick cases, the disk central temperature *is* dependent on the choice of α and K, as these affect the disk gas surface density and therefore τ (from eq. [9]). Makalkin et al. (1999) considered a restricted range of inflow rates and concluded that $\alpha \geq 10^{-3}$ would be needed to produce an appropriately cool disk. However, we show below that for any α (and K), there exist values of F_* that yield the required disk temperatures. Whether they are realistic or not must be determined by gas accretion models.

Figures 4 and 5 display predicted disk temperature profiles for two values of the inflow timescale, $\tau_G \equiv M_J/\dot{M}_J$, for the nominal model with $K = 10^{-4}$ cm^2 g^{-1}. For $\tau_G = 10^4$ yr (Fig. 4), temperatures are $\geq O(10^3)$ K throughout the regular satellite region even with $K = 10^{-4}$. A slower inflow rate yields a more appropriate disk temperature profile; Figure 5*c* shows $T_c(r)$ and $T_d(r)$ for $\tau_G = 5 \times 10^6$ yr and $\alpha = 5 \times 10^{-3}$. A disk pressure is estimated by $P = \mathcal{R}\rho_G T_c/\mu_{\rm mol}$; Figure 5*d* shows the implied temperature versus pressure profile. For low opacities and $\tau_G \geq 3 \times 10^6$ yr, disk conditions are consistent with ice stability exterior to Ganymede's orbit. The water-ice stability line shown in Figure 5*d* (from Prinn & Fegley 1989) should not be viewed as a sharp boundary, since the inflowing solids will be a mixture of ice and rock, and their survival against evaporation will be size-dependent. In addition, some inward migration of the satellites themselves likely occurred as a result of type I interaction with the disk (see § 3.5 and Figs. 7–9 below), so it is possible that they formed at somewhat greater orbital distances.

Figure 5*a* shows $\sigma_G(r)$ for $\tau_G = 5 \times 10^6$ yr with $\alpha = 5 \times 10^{-3}$. For a given inflow rate, $\sigma_G \propto 1/\alpha$, and even for a relatively low-viscosity disk [$\alpha \sim O(10^{-4})$], predicted gas surface densities for F_* slow enough for ice stability are orders of magnitude below the MMSN. In steady state, the total mass of gas with $r \leq r_c$ in Figure 5*a* is only $\sim$a few $\times 10^{25}$ g; for $r < r_c$, the radial surface density profile is approximately $\sigma_G \propto 1/r^{3/4}$. Figure 5*b* plots $(c/r\Omega)$ as a function of radius; in the inner disk, the disk aspect ratio increases gradually with radius, with $(c/r\Omega) \propto r^{1/8}$. In the outer disk $T_d \rightarrow T_{\rm neb}$ and the disk profile "flares" more rapidly with radius, with $(c/r\Omega) \propto r^{1/2}$.

In the case of a very high opacity disk ($K = 1$), even slower inflow rates are required to yield appropriately low disk temperatures. Figure 6 shows the resulting disk for $\tau_G = 10^8$ yr and $K = 1$. Midplane temperatures are somewhat high in this case for significant incorporation of ices near $\sim 15R_J$ (although inward migration of the satellites could ease this constraint; see Fig. 9). A somewhat broader and perhaps more likely range of inflow rates is possible assuming lower opacities and a less dust rich disk, which has been argued for previously (LS82).

A growth time of $\tau_G = 5 \times 10^6$ yr is orders of magnitude longer than that characteristic of runaway gas accretion, implying that the Galilean satellites formed as gas accretion onto Jupiter was abating, either as the nebula itself was dissipating or as inflow slowed as a result of Jupiter opening a gap. In the latter case, $\tau_G = 5 \times 10^6$ yr corresponds closely to that obtained by Bryden et al. (1999) for accretion through a gap onto Jupiter for a nebular viscosity alpha value of $\sim$a few $\times 10^{-4}$. This slow rate of gas accretion would need to persist for at least $\sim 0.02\tau_G \sim 10^5$ yr in order for a mass equal to the reconstituted mass of satellites to be processed through an appropriately low-temperature disk.

The inner disk properties are relatively insensitive to changes in the assumed outer edge of the disk. The value $r_d = 150R_J$ was motivated by the shocked regions seen in Lubow et al. (1999) and D'Angelo et al. (2002); a more generic choice would be the radius at which a disk of orbiting gas would begin to extend outside Jupiter's Hill sphere and thus be subject to removal via solar tides, or $r > 0.7R_H \sim 500R_J$. For the case shown in Figure 5, setting $r_d = 500R_J$ leads to an increase in σ_G by a few tens of percent for $r < r_c$ over that obtained with $r_d = 150R_J$. The steady-state gas surface densities are also not very sensitive to the choice of r_c.

3.4. *Evolution of Disk Solids*

In order to yield satellites from an accretion disk, solid material (rock + ice) must be supplied either by direct transport of small material into the disk with the gas inflow, or by capture of heliocentrically orbiting solids as they pass

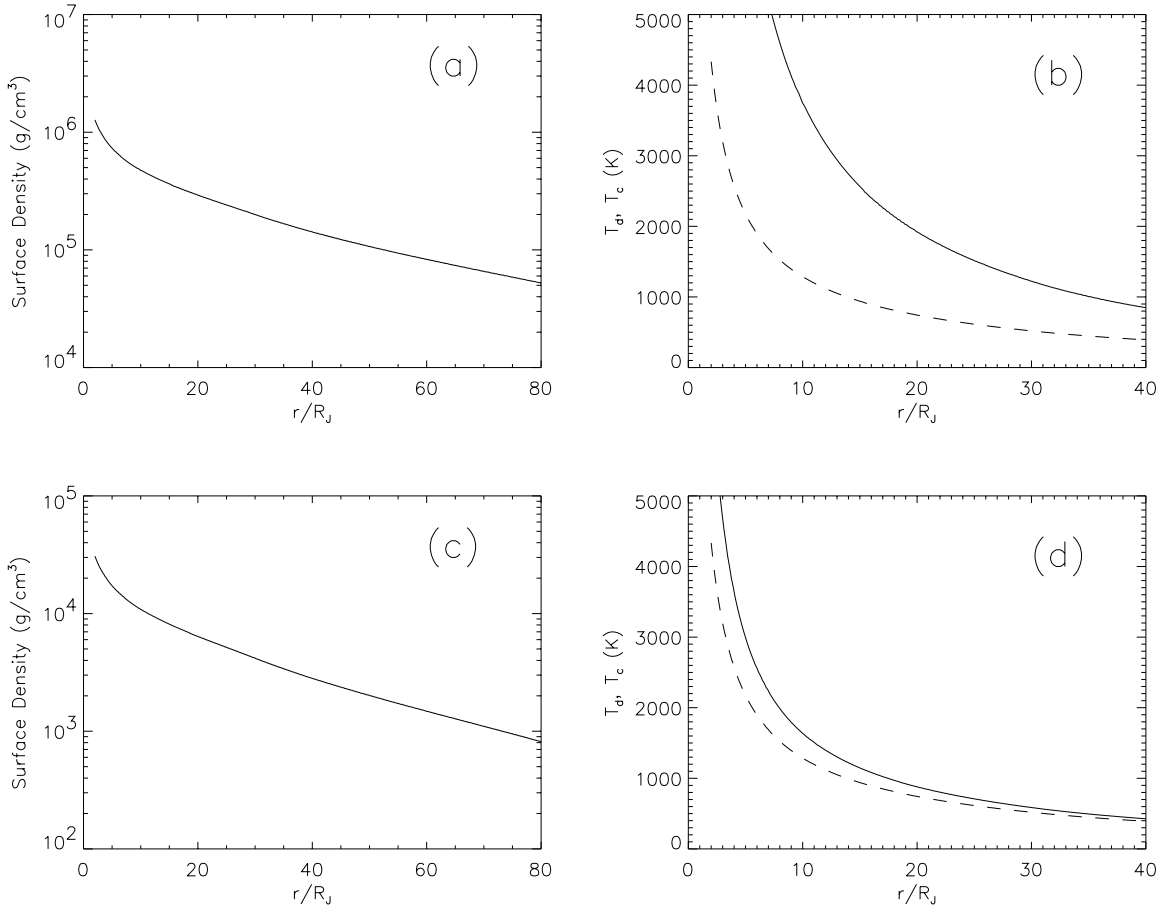

FIG. 4.—Disk steady-state surface densities and temperature profiles for a fast-inflow circumjovian accretion disk, with the nominal model and $\tau_G \equiv M_J/\dot{M}_J = 10^4$ yr and $K = 10^{-4}$ cm^2 g^{-1}. The disk midplane, T_c, and effective, T_d, temperatures are shown by the solid and dashed lines, respectively. (*a–b*) A low-viscosity disk, with $\alpha = 10^{-4}$, and (*c–d*) a high-viscosity disk with $\alpha = 0.01$. In both cases, resulting temperatures are too high for the incorporation of ices in the region of the regular satellites.

through the disk. A Sun-orbiting particle of radius R_s would have its motion dominated by the motion of the gas if its stopping time due to gas drag, t_e, is shorter than its orbital period (e.g., Weidenschilling & Cuzzi 1993), with $t_e \equiv R_s\rho_s/(c\rho_G) \ll 1/\Omega$, or

$$R_s \ll O(1)\ \mathrm{m}\left(\frac{2\ \mathrm{g\ cm^{-3}}}{\rho_s}\right)\left(\frac{\rho_G}{4\times10^{-11}\ \mathrm{g\ cm^{-3}}}\right) \times \left(\frac{c}{0.8\ \mathrm{km\ s^{-1}}}\right)\left(\frac{r}{5\ \mathrm{AU}}\right)^{3/2}, \quad (21)$$

where the nominal nebular values shown are for a minimum mass solar nebula at 5 AU with 150 K and $(H/r) = 0.07$. Thus, particles much smaller than ~1 m in radius would be expected be delivered to the accretion disk with the hydrodynamic gas inflow.

Once a circumplanetary disk has formed, solids could also be captured as a result of gas drag as they passed through the disk. This process would require that a traversing particle encounter a mass much greater than its own during passage through the disk, or

$$R_s \ll O(1)\ \mathrm{m}\left(\frac{\sigma_G}{500\ \mathrm{g\ cm^{-2}}}\right)\left(\frac{2\ \mathrm{g\ cm^{-3}}}{\rho_s}\right). \quad (22)$$

For disk surface densities appropriate to a slow inflow rate and $\alpha \geq 10^{-3}$, particles small enough to be captured as they pass through the disk would also be small enough to have had their motion dominated by the nebular gas motion (eq. [21]), and so would have likely instead been delivered to the disk with the inflowing gas. It is possible that both processes played some role in supplying disk solids, although if capture had been significant it is difficult to explain why a more extended regular satellite system would not have resulted.

It is uncertain what the appropriate gas-to-solid mass ratio of inflowing material would be; a nominal guess would be a solar ratio of $f_\odot \sim 10^2$, but this fraction could be larger if most of the mass in nebular solids at the end of Jupiter's growth is contained in larger sized planetesimals. However, some fraction of material at small sizes would be expected because of ongoing production during fragmenting planetesimal-planetesimal collisions, particularly given the potential collisional energetics at the edge of a Jovian-opened gap, from which most of the Hill entering material appears to originate (Lubow et al. 1999).

Solids delivered to the disk with the inflowing gas would achieve orbit around Jupiter at a similar orbital distance than that at which the gas achieved centrifugal balance, i.e., with $r < r_c$. The timescale for collisional accretion assuming some mass fraction of solids $1/f$ can then be compared to the disk's characteristic viscous time, to determine to what

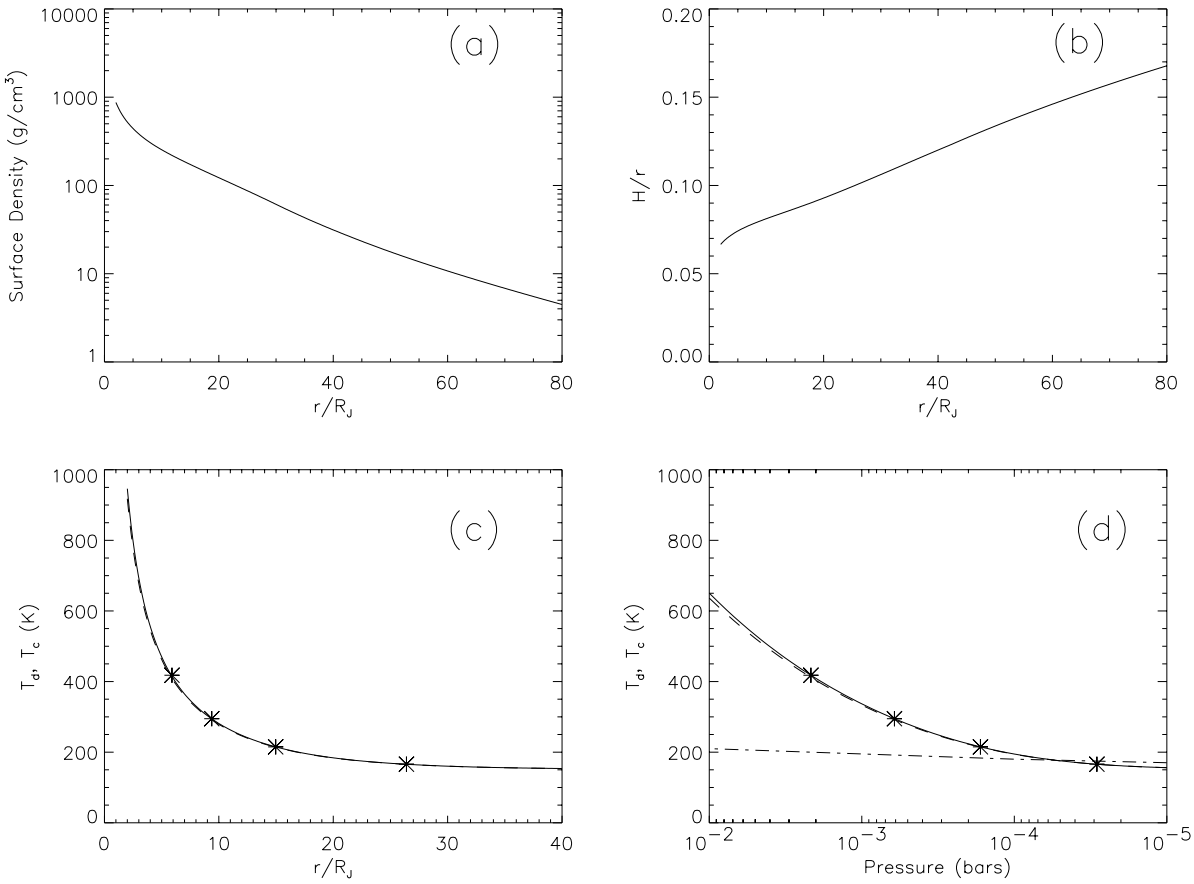

FIG. 5.—Predicted steady-state (*a*) surface density, (*b*) scale height, (*c*) temperature, and (*d*) temperature vs. midplane pressure profiles for a slow-inflow, low-opacity circumjovian accretion disk, with $\alpha = 5 \times 10^{-3}$, $\tau_G \equiv M_J/\dot{M}_J = 5 \times 10^6$ yr, $K = 10^{-4}$ cm^2 g^{-1}, and the nominal disk model (see Table 2). Disk midplane and effective temperatures are shown by the solid and dashed lines, respectively; positions of the current Galilean satellites are starred. The disk becomes isothermal (with $T_d = T_{\rm neb} = 150$ K) for $r \geq 40 R_J$. Shown in (*d*) is the water-ice stability curve (*dot-dashed line*) from Prinn & Fegley (1989), which is close to the predicted disk temperatures at the current locations of Ganymede and Callisto. For a fixed value of τ_G, the gas surface density is inversely proportional to α, as is the pressure. For the choice of K and τ_G shown here, the disk is optically thin (with $0.01 < \tau < 0.1$ in the region of the regular satellites), so that $T_d \approx T_c$, and a similar temperature profile results for any choice of α. Lower (higher) temperatures result for slower (faster) inflow rates.

extent particles could grow before being viscously removed from the disk, provided that turbulence is insufficient to prevent accretion. Setting $\tau_A = \tau_\nu$, with σ_G from equation (18) for $r < r_c$, and $\sigma_s = \sigma_G/f$ gives

$$R_s \sim O(10^2)\ \mathrm{m} \left(\frac{F_g}{10}\right)\left(\frac{100}{f}\right)\left(\frac{5\times10^{-3}}{\alpha}\right)^2\left(\frac{2\ \mathrm{g\ cm^{-3}}}{\rho_s}\right) \times \left(\frac{F_*}{M_J/5\times10^6\ \mathrm{yr}}\right)\left(\frac{15R_J}{r}\right)^{1/2}\left(\frac{0.1}{c/r\Omega}\right)^4 . \quad (23)$$

This estimate implies that once in circumplanetary orbit, objects large enough to decouple from the gas could collisionally aggregate on timescales much shorter than those on which they would be carried inward or outward with the gas disk as it viscously spread, over a wide range of f values.

Once having grown large enough to decouple from the gas disk, solids orbiting Jupiter would still interact with the gas through aerodynamic gas drag. The orbiting gas will be pressure-supported, so that the difference in its orbital velocity from Keplerian velocity is (e.g., Whipple 1972; Weidenschilling & Cuzzi 1993)

$$\Delta v_\theta \equiv v_K - v_G = -(2\rho_G\Omega)^{-1}\frac{dP}{dr} \sim c\left(\frac{c}{r\Omega}\right) . \quad (24)$$

For a disk with minimum temperature of ~150 K and $(c/r\Omega) \sim 0.1$, $\Delta v_\theta \geq 1$ km s^{-1}.[9]

The ratio of the accretion time to the lifetime against gas drag for a Jupiter-orbiting particle too small to gravitationally focus the gas (e.g., Ward 1993; Makalkin et al. 1999) is

$$\frac{\tau_A}{\tau_{\rm GD}} \sim 2\times10^{-3}\left(\frac{10}{F_g}\right)\left(\frac{f}{100}\right)\left(\frac{c/r\Omega}{0.1}\right)^3 . \quad (25)$$

Thus, objects would accumulate on timescales much shorter than their orbital decay time as a result of gas drag for a wide range of gas-to-solids ratios. We expect that solids delivered to the disk will rapidly accrete near to the radial distance at which they achieve centrifugal force balance, so that a region of accreting solids will exist for $R_J < r < r_c$. This implies that in order to account for the current location of the Galilean satellites, $r_c \sim 20$–$30\ R_J$; this range could be somewhat larger if some inward type I migration is accounted for (see § 3.5), perhaps $r_c \sim 35$–$40\ R_J$.

[9] In comparison, the radial inward/outward velocity of the circumjovian gas due to its viscous evolution is orders of magnitudes less, ~0.1–1 m s^{-1} for disk α values 10^{-3} to 10^{-2}.

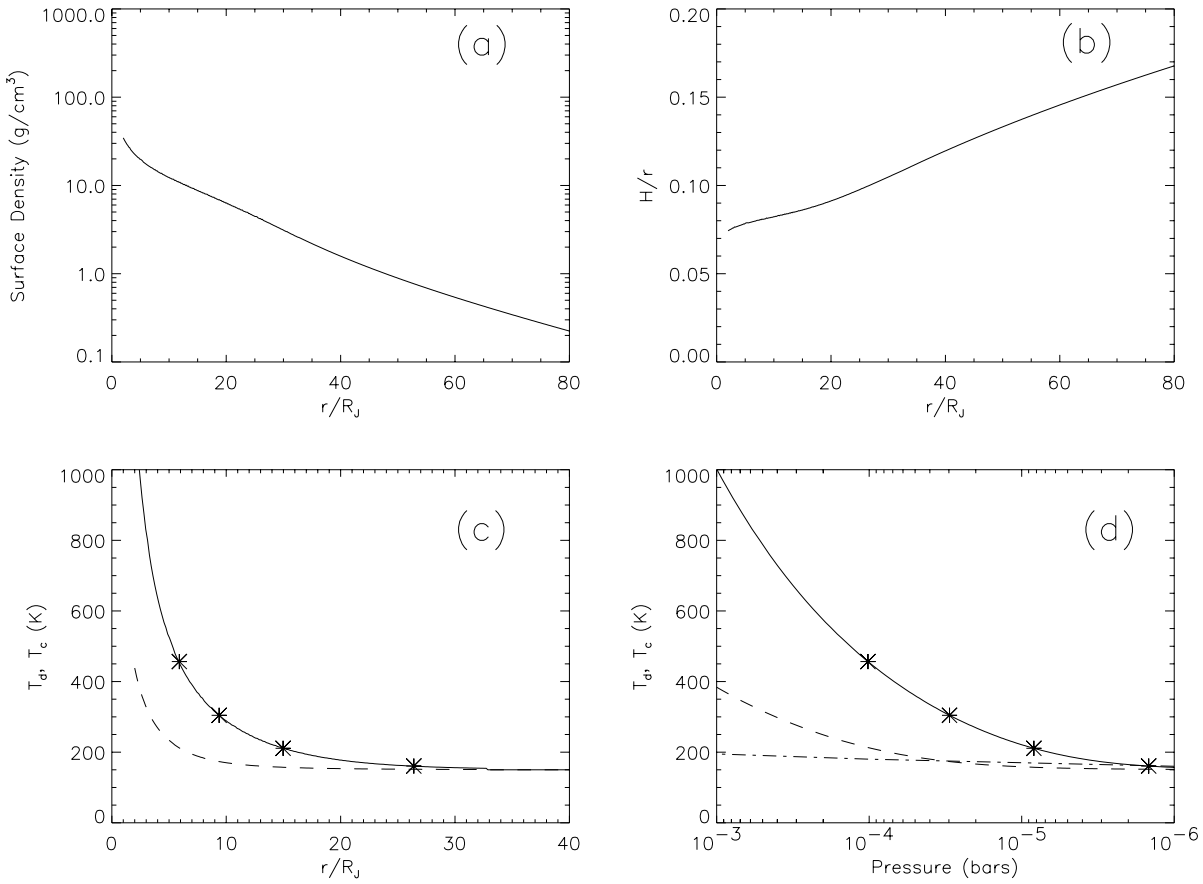

FIG. 6.—Predicted steady-state (*a*) surface density, (*b*) scale height, (*c*) temperature, and (*d*) temperature vs. midplane pressure profiles for an extremely slow inflow, high-opacity disk, with $\alpha = 5 \times 10^{-3}$, $\tau_G \equiv M_J/\dot{M}_J = 10^8$ yr, $K = 1$ cm^2 g^{-1}, and the nominal disk model. The disk is isothermal for $r \geq 25R_J$. Positions of the current Galilean satellites are starred. Predicted effective disk temperatures at Ganymede and Callisto's orbits are close to the water-ice stability curve; however, disk midplane temperatures at Ganymede are somewhat higher. For this choice of K, the resulting disk is optically thick, with $3 < \tau < 30$ in the region of the regular satellites.

As gas and solids are delivered to the disk, the gas then sustains a quasi–steady state, while the surface density of solids will build up over time. While the gas component of the disk viscously spreads outward and onto the planet, the solids rapidly accumulate in the region where they are initially delivered, providing a mechanism for accreting large satellites in a limited region extending from the surface of the planet to a characteristic distance, r_c, with the latter determined by the specific angular momentum of the inflowing material. This effective spatial fractionation of solids provides a means to explain why large satellites are not found at distances more commensurate with tidal stability, i.e., $\sim R_H$, as might be expected, e.g., in the spin-out model.

In the slow-inflow accretion disk, the overall formation time of the satellites is regulated by the time necessary to deliver an amount of solids M_S to the disk,

$$\tau_{\rm acc,in} = \tau_G f(M_S/M_J) \ , \qquad (26)$$

rather than by equation (1), with $\tau_{\rm acc,in} \geq 10^5$ yr for $\tau_G \geq 5 \times 10^6$ yr and $f = f_\odot$. For this accretion timescale, and in the limit that an accreting satellite forms from small material whose energy is deposited near to the satellite's surface, the balance of accreted versus radiated energy gives a surface temperature rise $\Delta T \leq 300$ K for a 2500 km radius satellite (Stevenson et al. 1986, Fig. 6), potentially consistent with an initial "cold start" for Callisto.

For the disk shown in Figure 5, the ratio of gas to solids in the region of the regular satellites decreases from $f = 10^2$ to $\leq O(1)$ in the time required to build up the satellites' combined mass in solids, implying that the final stages of satellite accretion occur in relatively gas-free conditions. This appears consistent with the results of Coradini et al. (1989), who calculated predicted satellite masses and spacing as a function of the protosatellite disk gas content using a feeding zone approximation; the best agreement with the Galilean satellites was obtained for a low-mass gas disk case.

3.5. *Satellite Migration and Survival*

From equation (3), the timescale for orbital decay of a large satellite due to type I interaction with the gas disk can be very rapid. In the cases favored here, the steady-state mass of the gas disk, M_d, is significantly less than $0.02M_J$, which acts to lengthen the migration timescale τ_I. However, the time necessary to accrete the satellites is also increased (eq. [26]), and so the consequences of potential satellite migration must still be addressed.

We first consider the dependence of the migration rate on satellite orbital radius. From equations (1), (18), and (20), the timescale for orbital decay due to type I interaction with

the disk increases with orbital radius, with[10]

$$\tau_{\rm I} \propto \frac{r^{1/2}}{M_S}\left[1-\frac{4}{5}\sqrt{\frac{r_c}{r_d}}-\frac{1}{5}\left(\frac{r}{r_c}\right)^2\right]^{-1}, \qquad (27)$$

where M_S is the satellite mass, $r < r_c$, and a viscosity-dominated energy production is assumed.[11]

The predicted rate of type I migration then increases as the orbital radius decreases, so that once a satellite began to migrate, its inward speed would continue to increase as it approached Jupiter. A dispersal of the gas or some other torque-modifying action would then be needed to halt a satellite's migration prior to its demise. A simple expectation for a satellite system that had undergone significant but incomplete migration might be to find a single exterior satellite—whose type I decay timescale had, e.g., exceeded the disk lifetime—with all massive interior satellites having been lost to inward decay. While this configuration is reminiscent of the Titan-dominated Saturnian system (Canup & Ward 2002b), it is quite distinct from the Galilean multiple satellite system.

In fact, the predicted type I decay timescales for the Galilean satellites are all quite similar (e.g., Figs. 7*b*, 8*b*, and 9*b*) given their current positions and masses. If these rates were more dissimilar, e.g., if $\tau_{\rm I}({\rm Callisto})/\tau_{\rm I}({\rm Io}) \gg 1$, then a formation history involving significant migration could be argued against by the very existence of the inner satellites. Instead, their similar type I timescales suggests that (1) they all migrated somewhat and were saved from destruction by the cessation of gas supply to the disk on a timescale $\leq$ their migration time, or (2) migration was insignificant for the disk conditions in which they formed. We consider both possibilities below.

A basic requirement for forming a satellite in the presence of type I torques is that $\tau_{\rm I} > \tau_{\rm acc,in}$, which places an upper limit on the gas surface density at the end of satellite forma-

[10] In equation (3) we considered an arbitrary surface density, while in equation (27) the radial surface density and temperature profiles are accounted for.

[11] The expression above is for full-strength interior and exterior disk torques acting on the satellites. Significant reflection off an inner boundary edge (e.g., the planetary surface) could reduce the interior torques for close-in satellites and act to increase their inward migration rate; similarly, reflection off an outer boundary edge could mitigate the exterior torques and lessen the tendency to migrate inward for outer satellites, although in § 2.2 we concluded that such a situation is unlikely for an expected outer disk edge profile.

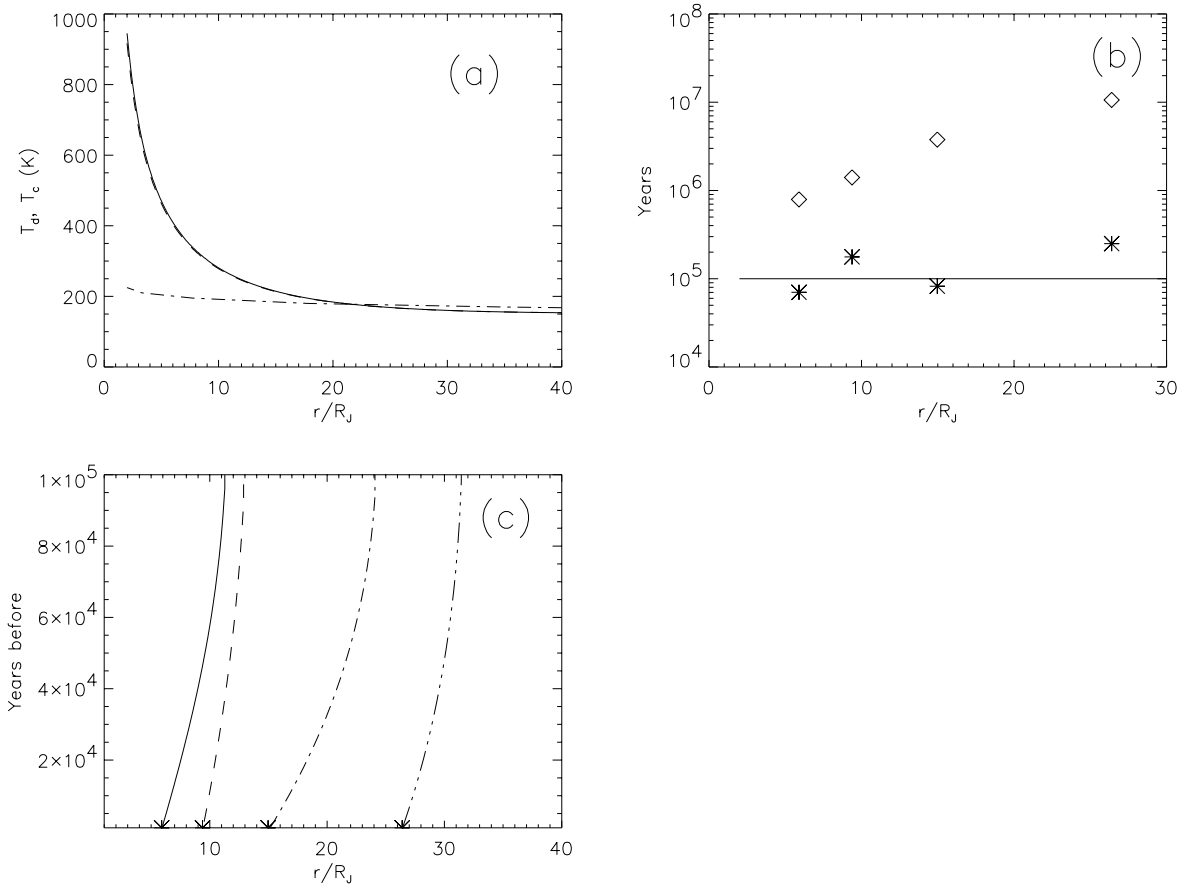

FIG. 7.—Slow-inflow, low-opacity steady-state disk, with $\alpha = 5 \times 10^{-3}$, $\tau_G \equiv M_{\rm J}/\dot{M}_{\rm J} = 5 \times 10^6$ yr, $K = 10^{-4}$ cm^2 g^{-1}, and the nominal disk model (same case as in Fig. 5). The temperature profile (with the solid line indicating midplane temperature, and the dashed line effective temperature) and the water-ice stability curve (*dot-dashed line*) are shown in (*a*). In (*b*) are plotted the type I and gas drag orbital decay timescales for the Galilean satellites with their current positions and masses (*stars and diamonds, respectively*), as well as the time required to deliver a mass in solids equal to the mass of the satellites to the disk, $\tau_{\rm acc,in}$ (*solid line*) for this value of τ_G. An estimated migration history for the satellites to end at their current locations is shown in (*c*), including effects due to gas drag and type I torques (assuming $C_a = 3.5$ and $C_D = 10$). The effect of a linear satellite growth in mass over time $\tau_{\rm acc,in}$ has been included. The type I timescales and migration histories assume full-strength torques, and that the satellites migrate independently.

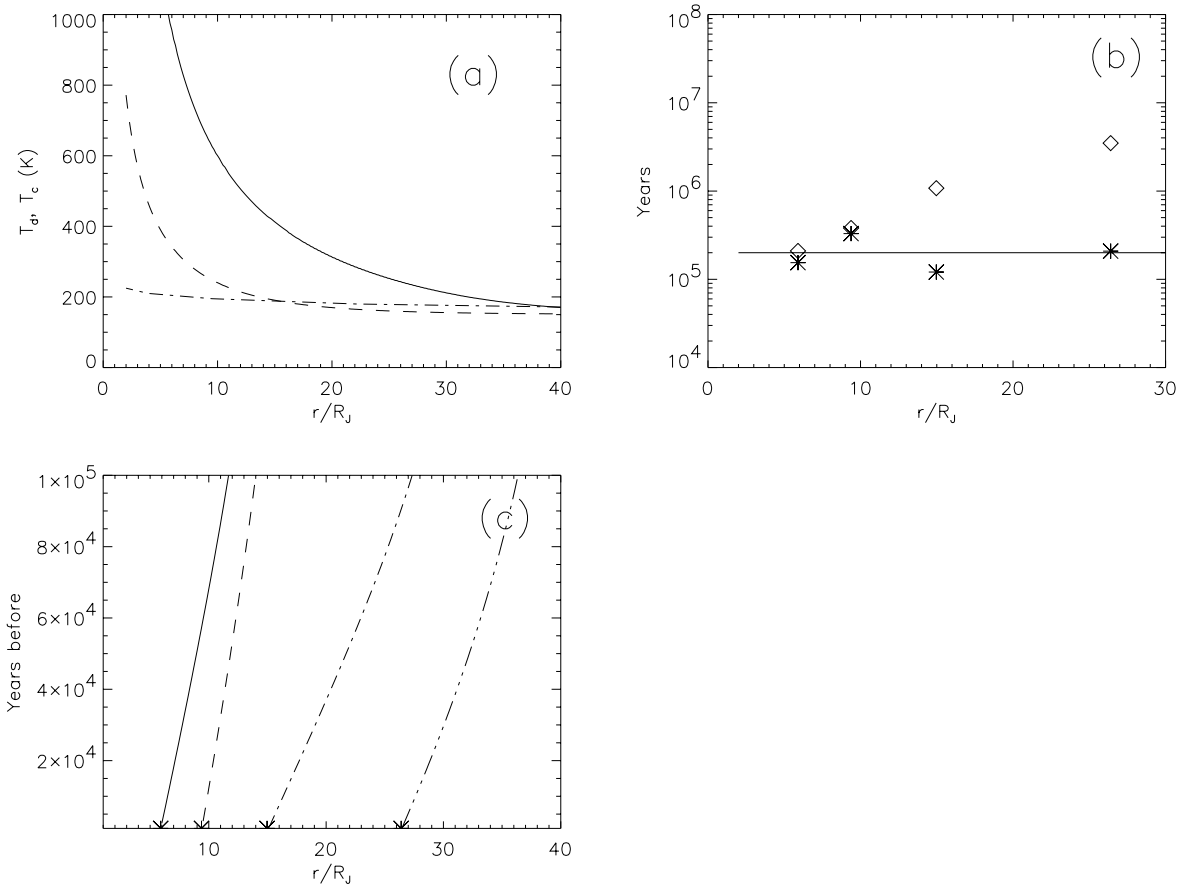

FIG. 8.—Same as Fig. 7, but here with $\alpha = 10^{-3}$, $\tau_G \equiv M_J/\dot{M}_J = 10^7$ yr, $K = 0.1$ cm^2 g^{-1}, and the nominal disk model

tion, and therefore a lower limit on the disk α-value. From (4), (19), and (27), for $r \leq r_c$,

$$\frac{\tau_I}{\tau_{\rm acc,in}} \approx \frac{3\pi}{fC_a}\left(\frac{M_J}{M_S}\right)^2\left(\frac{c}{r\Omega}\right)^4\alpha \approx O(1)\left(\frac{100}{f}\right)\left(\frac{c/r\Omega}{0.1}\right)^4\left(\frac{10^{26}\ \text{g}}{M_S}\right)^2\left(\frac{\alpha}{5\times10^{-3}}\right). \quad (28)$$

Assuming an inflow with $f = f_\odot$, type I migration would not have been significant over the satellite formation interval for a quite viscous protosatellite disk, i.e., with $\alpha \gg 10^{-2}$. For low disk viscosities, i.e., $\alpha \ll O(10^{-3})$, full-strength type I torques would preclude the formation and survival of Galilean-sized satellites.

Intermediate disk viscosities, with $O(10^{-3}) < \alpha < O(10^{-2})$, would yield some degree of inward migration during the satellite formation era. For example, with $\tau_G = 5 \times 10^6$ yr, $K = 10^{-4}$ cm^2 g^{-1}, and $\alpha = 5 \times 10^{-3}$ (the case shown in Fig. 5), Figure 7 shows the disk temperature profile and the water-ice stability line (Fig. 7*a*), and $\tau_{\rm acc,in}$, τ_I, and $\tau_{\rm GD}$ for the Galilean satellites (Fig. 7*b*). Figure 7*c* shows a satellite migration history, including effects due to both gas drag and type I torques, that would leave the satellites at their current positions after $t = \tau_{\rm acc,in}$. Here we have included the effect of a linear growth in satellite mass over this time period on the calculated $(da/dt)_{\rm I}$ and $(da/dt)_{\rm GD}$ rates and have assumed that each satellite's migration is independent. The latter would not be valid if the satellites were locked in mutual mean-motion resonances. Figure 8 shows the same for $\tau_G = 10^7$ yr, $\alpha = 10^{-3}$, and $K = 0.1$ cm^2 g^{-1}, and Figure 9 the same for the very slow inflow high-opacity case shown in Figure 6.

The inward differential type I migration of the satellites shown in Figures 7–9*c* could provide an opportunity for the establishment of the Laplace resonance from "outside-in" as Ganymede's larger mass causes its orbit to converge on that of both Europa and Io, providing an opportunity for resonance capture. Callisto is naturally omitted from this configuration because of its slower decay rate. Interestingly, Peale & Lee (2002) have recently demonstrated that the primordial origin of the Laplace resonance in this manner, combined with continuing tidal interaction with the planet after the subnebula has dissipated, can reproduce all of the features of the current configuration.

What general limits can be placed on the extent to which the satellites could have migrated inward, and thus on their formation in a somewhat more exterior (and thus typically colder for a given inflow rate) region of the disk? While Ganymede could have captured Europa and Io into mean-motion resonances as it migrated inward, the orbits of Ganymede and Callisto diverge, and thus these satellites would have been closer together in the past. A crude estimate for the upper limit on the degree of migration can then be determined by back-tracking their orbits until they were marginally stable, with $(a_C - a_G) = 3.5R_H = 3.5a_G[(M_G + M_C)/3M_J]^{1/3}$, or $a_G/a_C \approx 0.9$. Assuming a mass ratio between the two satellites similar to the current

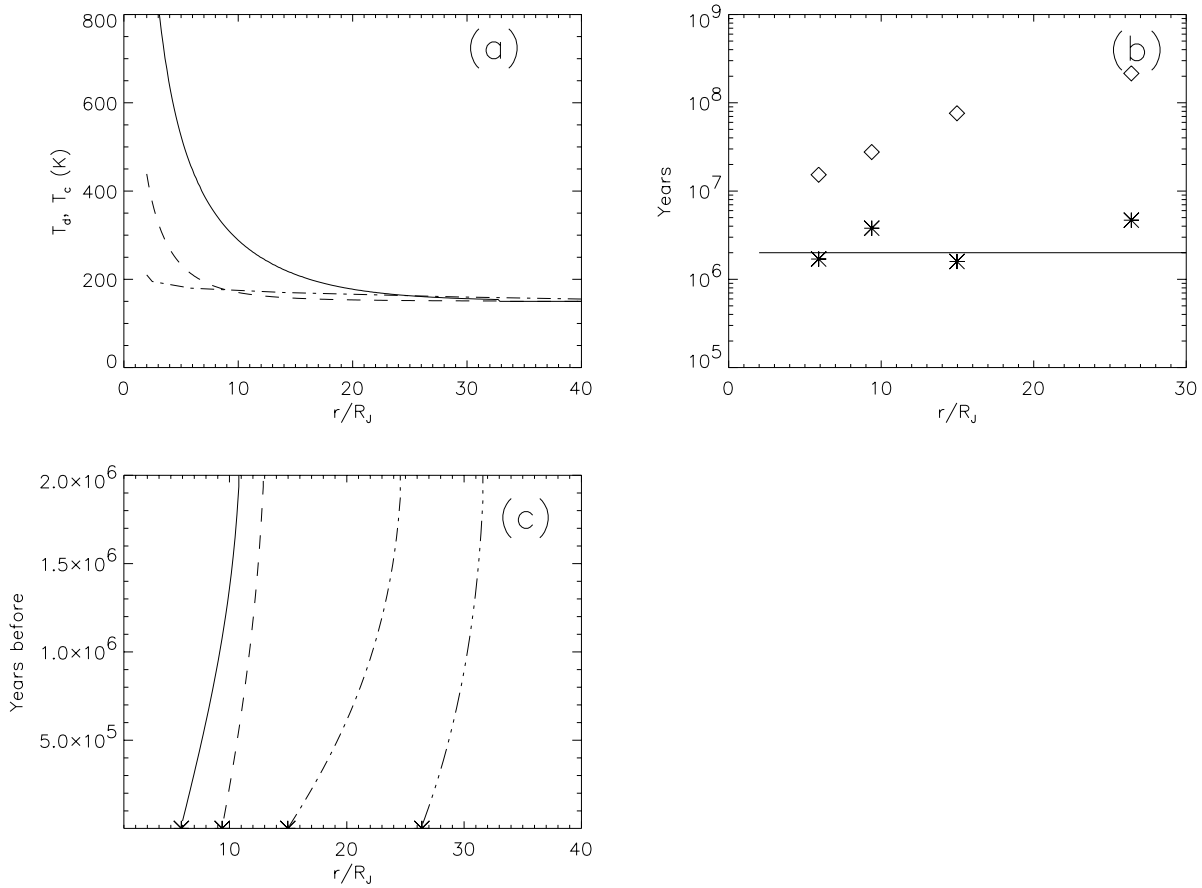

FIG. 9.—Same as Figs. 7 and 8, with $\alpha = 5 \times 10^{-3}$, $\tau_G \equiv M_J/\dot{M}_J = 10^8$ yr, $K = 1$ cm^2 g^{-1}, and the nominal disk model (same case as in Fig. 6)

one, this implies that Callisto could not have migrated in from greater than about $35R_J$ (assuming that this region of the disk would have been isothermal), while Ganymede would have needed to form within about $30R_J$.

In a moderate-migration scenario, somewhat higher rates of inflow for a given disk opacity could then be consistent with an ice-rich Ganymede, since the satellite could form in a somewhat more exterior portion of the disk. For example, ice stability exterior to $30R_J$ in the low-opacity disk shown in Figure 5 requires $\tau_G \geq 10^6$ yr, while for the high-capacity case shown in Figure 6, $\tau_G \geq 5 \times 10^7$ yr is needed.

We note that for satellite formation from a "gas-starved" disk, the build-up of the appropriate mass in solids occurs over multiple disk viscous cycles, implying that satellites massive enough to open gaps would be lost due to type II decay, which would occur on a viscous timescale with $\tau_\nu \ll \tau_{\rm acc,in}$. It may not be coincidental that the Galilean satellites fall quite near in mass to that required to open a gap from equation (5), as more massive satellites might not survive. It is also plausible that earlier generations of satellites accreted during periods of more rapid gas inflow onto Jupiter and were lost to either type I or II decay to the planet, so that the Galileans were simply the last generation of satellites to form and survive. Satellites forming during periods of higher gas inflow would have been more rock-rich than the Galileans for $r \leq r_c$, given the higher predicted disk temperatures. Alternatively, it may be that the Galileans were the only substantial satellite system to form; e.g., it is possible that only during the very last phase of its growth did Jupiter contract sufficiently to allow for the formation of a circumplanetary accretion disk.

4. SUMMARY AND DISCUSSION

The standard model holds that the Galilean satellites formed from a disk containing their total mass in solids, augmented in gaseous components to match the bulk solar composition. Formation from the implied gas-rich, $0.02M_J$ "minimum-mass subnebula" (MMSN) presents multiple difficulties for Galilean satellite formation and survival, including

1. Rapid accretion times for all four satellites $\leq 10^3$ yr, in apparent contradiction with the long, $>10^5$ yr formation times implied by Callisto's partially differentiated state.
2. Disk temperatures too high for ices in the region of Ganymede and Callisto unless the disk is extremely inviscid (requiring $\alpha \leq 10^{-6}$ using a Shakura and Sunyaev α viscosity parameterization), with a correspondingly long disk viscous lifetime of $\gtrsim 10^6$ yr.
3. Extremely short lifetimes of Galilean-sized satellites against type I orbital decay due to disk torques ($\sim 10^2$ yr) and aerodynamic gas drag ($\sim 10^3$ yr), in contradiction to satellite survival given the disk lifetimes implied by point 2.
4. Loss of satellites due to type II decay on a timescale of $\sim O(1/\alpha)$ yr if the satellites are able to open gaps in the disk. Survival of satellites in gaps would require the disk to be removed by a nonviscous means, e.g., via photoevapora-

tion, which would then necessitate an even longer disk lifetime of $\sim 10^7$ yr and a lower viscosity, $\alpha \leq 10^{-7}$.

5. The effective viscosity imposed by a Galilean-sized satellite as a result of its density wave interaction with the disk implies $\alpha \sim 10^{-4}$–10^{-3}, in contradiction to both points 2 and 4.

6. If the satellite-induced viscosity from point 5 could be avoided through the opening of wide gaps, Galilean-sized satellites occupying such gaps would have their eccentricities excited by first-order Lindblad resonances on timescales of only $\sim 10^3$ yr, making the orbital stability for 10^7 yr required by point 4 difficult to reconcile.

7. A key independent trait—Jupiter's current very low obliquity—provides strong circumstantial evidence against the existence of a long-lived MMSN circumjovian disk. If such a massive disk had been present after removal of the solar nebula, Jupiter would likely have passed through a resonance involving its spin precession rate and the ν_{16} orbital precession frequency as the circumplanetary disk dissipated (Ward & Hamilton 2002). Such a passage would have generated an obliquity significantly larger than $\theta \approx 3^\circ$.

We instead find that a self-consistent, and much less restrictive, scenario results by considering satellite formation in a circumjovian accretion disk produced during the slowing of gas inflow onto Jupiter. The creation of such a disk is supported by results of recent hydrocode simulations of gas accretion onto Jupiter at the end stages of the planet's growth and as the planet has opened a gap in the nebular disk (e.g., Lubow et al. 1999; D'Angelo et al. 2002). In such a model:

1. Gas inflow rates of a Jovian mass in $\geq$ a few $\times 10^6$ yr yield disk temperatures sufficiently low to allow for ice stability in orbits exterior to that of Ganymede, and for hydrated silicates in the region of Europa. Varying the assumed values of disk opacity and assumed viscosity alpha parameters affects the required inflow time for a given case, but successful models can be found over a wide range of these parameters.

2. Given the temperature requirements in point 1, the resulting steady-state circumplanetary gas disk is orders of magnitude less massive than the minimum-mass subnebula model. In many cases, this "gas-starved" disk is optically thin.

3. Over a wide range of assumed gas-to-solid ratios in the inflowing material, disk solids will rapidly accumulate once they are placed into orbit, decoupling from the gas disk and growing faster than they can be removed via gas drag. The mass of solids and the solid-to-gas ratio in the disk thus increase with time, so that the final stages of satellite growth occur in a relatively gas-free and low-pressure environment.

4. The overall formation time of the satellites is controlled by the inflow timescale of the solar nebula material, rather than the satellites' short orbital timescales. Thus, long satellite accretion times of $\geq 10^5$ yr—such as that apparently needed to account for Callisto—result for the inflow rates implied by point 1.

5. Satellite survival against type I decay for the formation interval in point 4 is predicted if the disk viscosity alpha parameter is $\alpha \geq 10^{-3}$ for inflowing material with a solar gas-to-solids ratio.

6. Disk viscosities with $O(10^{-3}) < \alpha < O(10^{-2})$ yield inward migration of Galilean-sized satellites during the satellite formation era as a result of type I torques. The differential migration rates provide an alternative means of establishing the Laplace resonance among the inner three satellites (Peale & Lee 2002).

7. Satellite formation occurs during Jupiter's accretion of the final few percent of its mass. The circumplanetary disk is removed as gas inflow to Jupiter stops, presumably as the nebula itself dissipates. Once inflow ceases, the gas disk is viscously removed on a timescale of $\sim O(1/\alpha)$ yr, or $\leq 10^3$ yr from point 5.

Thus, given current understanding of giant planet growth and satellite-disk interactions, we believe that the formation of the Galilean satellites from a "gas-starved" accretion disk is strongly favored over formation from a gas-rich MMSN disk. This implies that satellite formation occurred within a much lower gas density environment than considered by previous models for satellite growth (e.g., Lunine & Stevenson 1982; Coradini et al. 1989) and Jovian subnebular chemistry (Prinn & Fegley 1981, 1989).

Several key aspects of the accretion disk model are uncertain and merit further investigation. In order to account for the radial scale of the Jovian regular satellite system, the inflowing material should be characterized by some maximum prograde specific angular momentum, $j \leq (GM_J r_c)^{1/2}$, so that it achieves centrifugal force balance orbiting Jupiter interior to $25R_J \leq r_c \leq 35R_J$, with this value depending on the amount of inward migration of the satellites via point 6 above. This corresponds to $j \leq (0.3\text{–}0.4)\Omega_J R_H^2$, expressed in terms of Jupiter's orbital frequency and Hill radius. It appears likely that the next generation of hydrocode simulations will have sufficient resolution to test this requirement. In addition, models of the late growth of Jupiter that self-consistently account for the planet's contraction could address whether the inflow rates implied in point 1 are consistent with a Jovian radius smaller than the current satellite system.

Recent N-body accretion simulations suggest that a satellite system similar in mass and number to that of the Jovian system could result from a gas-free disk with a mass and angular momentum similar to that contained in the satellites (Canup & Ward 2000). However, in the model favored here, satellite growth will be regulated by a slow inflow of material. It is possible that in an inflow-regulated disk, the protosatellite system at a given time would appear as a distribution of satellites, sufficiently separated in orbital distance to maintain short-term stability (e.g., 5–10 mutual Hill radii). Inflowing material accreting onto the satellites would gradually increase their mass until the point of system destabilization, collisions, and ultimately a decrease in the number of satellites. The potential for such an episodic growth pattern has not been explored previously, and will be a focus of our future work. Indeed, the distribution of resulting satellites could provide constraints on the required radial dependence of the inflow flux, which was assumed to be uniform in this work.

In the absence of such detailed accretion studies, we note that the gas-starved disk model predicts long accretion times for all of the Galilean satellites. There are other factors that could have contributed to the greater observed degree of resurfacing and differentiation on Ganymede than that seen on Callisto. First, Ganymede

may have been tidally heated as a result of its involvement in orbital resonances subsequent to its formation (e.g., Showman et al. 1997; cf. Peale 1999). Second, Ganymede is somewhat more massive, and would have likely formed in a higher subnebula temperature environment. Assuming a gas-free accretion scenario and a low value for the fraction of heat deposited at depth in the satellite per accretional impact (which seems plausible for accretion of predominantly small, inflowing solids), Ganymede and Callisto can fall on opposite sides of the water-melting curve (e.g., Stevenson et al. 1986). An important test of the gas-starved disk model will be how well it can fit into a more detailed scenario for the origin of the Ganymede-Callisto dichotomy. Another issue concerns the accretion of rock versus ice during the final stages of growth of these two large satellites, as accreting ices may upon initial impact be sublimed or vaporized, since the gravitational potential energy per unit mass at this point is roughly the latent heat of sublimation of water. Assuming that the ambient subnebula temperature and pressure still fall below the water-ice stability curve, it seems likely that this material would recondense while still in Jovian orbit and reaccrete onto the satellites, so that the net accreting material would have a similar rock-to-ice ratio as that in the inflowing solids. However, this point deserves a closer examination as well.

The similarities in the believed growth processes of Jupiter and Saturn, as well as in the features of their satellite systems, suggest that a common mode of origin produced the regular satellites of both planets. We are beginning to explore the ramifications of a slow-inflow–produced accretion disk model and type I migration for the Saturnian system (Canup & Ward 2002b).[12] We hope that continued study of satellite origin in both the Jupiter and Saturn systems can provide valuable constraints on the late-stage growth of gas giant planets and related nebular conditions, as well as the specific formation histories that set the conditions for satellite chemical inventories, thermal history, and later dynamical evolution.

We wish to acknowledge helpful discussion with D. Stevenson at the 2001 Jupiter Conference in Boulder, CO; his talk at that meeting included some concepts similar to those we presented, and which are explored further here. We thank S. Peale for sharing some unpublished results with us on the establishment of the Laplace resonance via inward orbital migration. The manuscript benefited from constructive comments from an anonymous reviewer, D. Hamilton, S. Peale, A. Stern, and J. Wisdom. This research was supported by NASA's Planetary Geology and Geophysics Program.

Correspondence and requests for materials should be addressed to R. M. C. (robin@boulder.swri.edu).

[12] Titan is intermediate in mass between Ganymede and Callisto and its degree of differentiation is uncertain, but differentiation exceeding that of Callisto is not necessarily inconsistent with long accretion times for Titan similar to those found here. It has been suggested (e.g., Schubert et al. 1986; Stevenson et al. 1986) that lower ambient nebular temperatures at Saturn likely allowed for the incorporation of the more volatile ammonia-water ice and clathrate hydrate, which could act to reduce the freezing temperature and increase the degree of expected melting in that environment (also Coradini et al. 1989).

APPENDIX

After Lynden-Bell & Pringle (1974), we consider a gas protosatellite disk with viscosity ν and surface density σ_G, in which shearing stress causes a viscous couple

$$g(r) = 3\pi\sigma_G h\nu \tag{A1}$$

on material in the disk orbiting at radius r with specific angular momentum $h = \Omega r^2$. For a fixed central gravity field,

$$F\frac{dh}{dr} = -\frac{\partial g}{\partial r}\ , \tag{A2}$$

where $F = 2\pi\sigma_G r u$ is the flux of material moving outward with velocity u through radius r.

We desire a quasi–steady-state solution for $F(r)$ and $\sigma_G(r)$ as a function of the inflow supply to the disk. We assume that inflowing material to the disk is characterized by a specific angular momentum, j, in the range of $(GM_J R_J)^{1/2} \le j_{\rm in} \le (GM_J r_c)^{1/2}$ (e.g., Cassen & Summers 1983; Coradini & Magni 1984; Makalkin et al. 1999), so that material is deposited into centrifugally supported orbits with a uniform flux per area $F_{\rm in}$ in the region extending to the radial distance r_c. The total infalling flux is then just $F_* = \pi F_{\rm in} r_c^2$. It is further assumed that there is a disk outer edge, r_d, at which point material is removed from the circumplanetary system and $g(r_d) = 0$, and that the viscous couple at the planet's surface, r_p, also vanishes, $g(r_p) = 0$.

From the continuity equation for a disk in steady-state,

$$\frac{\partial\sigma_G}{\partial t} = \frac{-1}{2\pi r}\frac{dF}{dr} + F_{\rm in} = 0\ ,$$
$$\frac{dF}{dr} = 2\pi r F_{\rm in}\ . \tag{A3}$$

Since $F_{\rm in} = 0$ for $r > r_c$, the flux of material moving outward in the disk exterior to r_c is $F(r > r_c) = F_0 =$ constant, and from equation (A2),

$$F_0[h(r > r_c) - h_d] = -[g(r > r_c) - g_d] = -g(r > r_c)\ , \tag{A4}$$

where the subscript d corresponds to values at the disk outer edge, r_d. Interior to r_c, $F = F(r)$ because material is being added to the disk across a range of radii. Substituting $F\,dh/dr = d/dr(Fh) - h\,dF/dr$ into equation (A2) and integrating gives

$$hF(r) + g(r) = \tfrac{4}{5}\pi r^2 h F_{\rm in} + A\ , \tag{A5}$$

where A is a constant, defined by the boundary condition $g(R_p) = 0$ to be $A = F_p h_p - \frac{4}{5}\pi F_{\rm in} r_p^2 h_p$.

The condition that F must be continuous at $r = r_c$ requires that $F(r_c) = F_0$, which when combined with equations (A4) and (A5) gives

$$F_0 h_d - F_p h_p = \tfrac{4}{5}\pi F_{\rm in}(r_c^2 h_c - r_p^2 h_p)\ . \tag{A6}$$

From conservation of mass, the sum of the magnitudes of the flux onto the planet and that flowing outward past r_d must equal the total inflowing flux to the disk; combining $|F_p| + |F_0| = F_* - \pi F_{\rm in} R_J^2$ with equation (A6) gives the

steady-state flux exterior to r_c,

$$F(r > r_c) = F_0 = \pi F_{\rm in} r_c^2 \left[\frac{4}{5}\left(\frac{r_c}{r_p}\right)^{1/2} + \frac{1}{5}\left(\frac{r_p}{r_c}\right)^2 - 1\right] \times \left[\left(\frac{r_d}{r_p}\right)^{1/2} - 1\right]^{-1} . \quad \text{(A7)}$$

Interior to r_c, the inward flux past each radius r must equal the difference between the total supply flux exterior to r minus the outward flux F_0; since we have defined $F < 0$ to be an inflowing flux, this translates to the condition that

$$-F(r) = \int_r^{r_c} 2\pi r F_{\rm in}\, dr - F_0 , \quad \text{(A8)}$$

which in combination with equation (A7) gives the steady-state flux interior to r_c,

$$F\ (r < r_c) = -\pi F_{\rm in} r_c^2 \times \left[1 - \left(\frac{r}{r_c}\right)^2 - \frac{(4/5)\left(r_c/r_p\right)^{1/2} + (1/5)\left(r_p/r_c\right)^2 - 1}{\left(r_d/r_p\right)^{1/2} - 1}\right] . \quad \text{(A9)}$$

For the cases of interest here, $(r_p/r_c)^2 \ll 1$ and $(r_d/r_p)^{1/2} \gg 1$, the steady-state fluxes then reduce to

$$F(r \geq r_c) = F_0 \approx F_* \left[\frac{4}{5}\left(\frac{r_c}{r_d}\right)^{1/2}\right] ,$$

$$F(r < r_c) \approx -F_* \left[1 - \left(\frac{r}{r_c}\right)^2 - \frac{4}{5}\left(\frac{r_c}{r_d}\right)^{1/2}\right] , \quad \text{(A10)}$$

and the flux onto the planet is

$$F_p \approx -F_* \left[1 - \frac{4}{5}\left(\frac{r_c}{r_d}\right)^{1/2}\right] . \quad \text{(A11)}$$

The fluxes in equation (A10), together with equations (A4) and (A5), yield the steady-state disk gas surface density:

$$\sigma_G(r) \approx \frac{4F_*}{15\pi\nu} \begin{cases} \frac{5}{4} - \sqrt{\frac{r_c}{r_d}} - \frac{1}{4}\left(\frac{r}{r_c}\right)^2 & \text{for } r < r_c , \\ \sqrt{\frac{r_c}{r}} - \sqrt{\frac{r_c}{r_d}} & \text{for } r \geq r_c . \end{cases} \quad \text{(A12)}$$

REFERENCES

Adachi, I., Hayashi, C., & Nakazawa, K. 1976, Prog. Theor. Phys., 56, 1756
Agnor, C. B., & Ward, W. R. 2002, ApJ, 567, 579
Anderson, J. D., Lau, E. L., Sjogren, W. L., Schuber, G., & Moore, W. B. 1996, Nature, 384, 541
Anderson, J. D., Jacobson, R. A., McElrath, T. P., Moore, W. B., Schubert, G., & Thomas, P. C. 2001, Icarus, 153, 157
Applegate, J. H., Douglas, M. R., Gursel, Y., Sussman, G. J., & Wisdom, J. 1986, AJ, 92, 176
Artymowicz, P. 1993, ApJ, 419, 166
Bodenheimer, P., Grossman, A. S., Decampli, W. M., Marcy, G., & Pollack, J. B. 1980, Icarus, 41, 293
Bodenheimer, P., Hubickyj, O., & Lissauer, J. 2000, Icarus, 143, 2
Bodenheimer, P., & Pollack, J. B. 1986, Icarus, 67, 391
Bryden, G., Chen, X., Lin, D. N. C., Nelson, R. P., & Papaloizou, J. C. B. 1999, ApJ, 514, 344
Burrows, A., Hubbard, W. B., Lunine, J. I., & Liebert, J. 2001, Rev. Mod. Phys., 73, 719
Burrows, A., Marley, M., Hubbard, W. B., Lunine, J. I., Guillot, T., Saumon, D., Freedman, R., Sudarsky, D., & Sharp, C. 1997, ApJ, 491, 856
Cabot, W., Canuto, V. M., Hubickyi, O., & Pollack, J. B. 1987, Icarus, 69, 387
Canup, R. M., & Ward, W. R. 2000, BAAS, 32, 5501
———. 2002a, Paper presented at Jupiter Conference, Boulder CO (http://lasp.colorado.edu/jupiter)
———. 2002b, BAAS, 33, 1405
Cassen, P., & Summers, A. 1983, Icarus, 53, 26
Chiang, E. I., Joung, M. K., Creech-Eakman, M. J., Qi, C., Kessler, J. E., Blake, G. A., & van Dishoeck, E. F. 2001, ApJ, 547, 1077
Coradini, A., Cerroni, P., Magni, G., & Federico, C. 1989, in Origin and Evolution of Planetary and Satellite Atmospheres, ed. S. K. Atreya, J. B. Pollack, & M. S. Matthews (Tucson: Univ. Arizona Press), 723
Coradini, A., & Magni, G. 1984, Icarus, 59, 376
D'Angelo, G., Henning, T., & Kley, W. 2002, A&A, 385, 647
Friedson, A. J., & Stevenson, D. J. 1983, Icarus, 56, 1
Goldreich, P., & Sari, R. 2002, ApJ, submitted
Goldreich, P., & Tremaine, S. 1979, ApJ, 233, 857
———. 1980, ApJ, 241, 425
Goodman, J., & Rafikov, R. R. 2001, ApJ, 552, 793
Harris, A. W., & Ward, W. R. 1982, Ann. Rev. Earth Planet Sci., 10, 61
Hayashi, C., Nakazawa, K., & Nakagawa, Y. 1985, in Protostars and Planets II, ed. D. C. Black & M. S. Matthews (Tucson: Univ. Arizona Press), 1100
Henrard, J., & Murigande, C. 1987, Celest. Mech., 40, 345
Hollenbach, D. J., Yorke, H. W., & Johnstone, D. 2000, in Protostars and Planets IV, ed. V. Mannings, A. P. Boss, & S. S. Russell (Tucson: Univ. Arizona Press), 401
Hourigan, K., & Ward, W. R. 1984, Icarus, 60, 29
Hubbard, W. B., Burrows, A., & Lunine, J. I. 2002, ARA&A, submitted
Ikoma, M., Nakazawa, K., & Emori, H. 2000, ApJ, 537, 1013
Kley, W., D'Angelo, G., & Henning, T. 2001, ApJ, 547, 457
Korycansky, D. G., Bodenheimer, P., & Pollack, J. B. 1991, Icarus, 92, 234
Lewis, J. S. 1974, Science, 186, 440
Lin, D. N. C., & Papaloizou, J. C. B. 1986, ApJ, 307, 395
Lin, D. N. C., Papaloizou, J. C. B., Terquem, C., Bryden, G., & Ida, S. 2000, in Protostars and Planets IV, ed. V. Mannings, A. P. Boss, & S. S. Russell (Tucson: Univ. Arizona Press), 1111
Lissauer, J. J., & Stewart, G. R. 1993, in Protostars and Planets III, ed. E. H. Levy & J. I. Lunine (Tucson: Univ. Arizona Press), 1061
Lubow, S. H., Bate, M. R., & Ogilvie, G. I. 2002, in preparation
Lubow, S. H., Seibert, M., & Artymowicz, P. 1999, ApJ, 526, 1001
Lunine, J. I., & Stevenson, D. J. 1982, Icarus, 52, 14 (LS82)
Lynden-Bell, D., & Pringle, J. E. 1974, MNRAS, 168, 603
Makalin, A. B., Dorofeeva, V. A., & Ruskol, E. L. 1999, Sol. Syst. Res., 33, 578
McKinnon, W. B. 1997, Icarus, 130, 540
Mizuno, H. 1980, Prog. Theor. Phys., 64, 544
Mosquiera, I., Estrada, P. R., Cuzzi, J. N., & Squyres, S. W. 2001, Lunar Planet. Sci. Conf., 32, 1989
Ohtsuki, K., Nakagawa, Y., & Nakazawa, K. 1988, Icarus, 75, 552
Papaloizou, J. C. B., & Larwood, J. D. 2000, MNRAS, 315, 823
Peale, S. J. 1999, ARA&A, 37, 533
Peale, S. J., & Lee, M. H. 2002, Nature, submitted
Pollack, J. B., & Bodenheimer, P. 1989, in Origin and Evolution of Planetary and Satellite Atmospheres, ed. S. K. Atreya, J. B. Pollack, & M. S. Matthews (Tucson: Univ. Arizona Press), 564
Pollack, J. B., & Consolmagno, G. 1984, in Saturn, ed. T. Gehrels & M. S. Matthews (Tucson: Univ. Arizona Press), 811
Pollack, J. B., Hubickyj, O., Bodenheimer, P., Lissauer, J. J., Podolack, M., & Greenzweig, Y. 1996, Icarus, 124, 62
Pollack, J. B., Lunine, J. I., & Tittemore, W. C. 1991, in Uranus, ed. J. T. Bergstralh, E. D. Miner, & M. S. Matthews (Tucson: Univ. Arizona Press), 469
Prinn, R. G., & Fegley, B., Jr. 1981, ApJ, 249, 308
———. 1989, in Origin and Evolution of Planetary and Satellite Atmospheres, ed. S. K. Atreya, J. B. Pollack, & M. S. Matthews (Tucson: Univ. Arizona Press), 78
Quillen, A. C., & Trilling, D. E. 1998, ApJ, 508, 707
Ruskol, E. L. 1982, Izvestiva Earth Phys., 18, 425
Schubert, G., Spohn, T., & Reynolds, R. T. 1986, in Satellites, ed. J. A. Burns & M. S. Matthews (Tucson: Univ. Arizona Press), 224
Schwarzschild, M. 1958, Structure and Evolution of the Stars (New York: Dover)
Shakura, N. I., & Sunyaev, R. A. 1973, A&A, 24, 337
Showman, A. P., Stevenson, D. J., & Malhotra, R. 1997, Icarus, 129, 367
Stevenson, D. 2001, Science, 294, 71

Stevenson, D. J., Harris, A. W., & Lunine, J. I. 1986, in Satellites, ed. J. A. Burns & M. S. Matthews (Tucson: Univ. Arizona Press), 39
Stone, J. M., Gammie, C. F., Balbus, S. A., & Hawley, J. F. 2000, in Protostars and Planets IV, ed. V. Mannings, A. P. Boss, & S. S. Russell (Tucson: Univ. Arizona Press), 589
Tajima, N., & Nakagawa, Y. 1997, Icarus, 126, 282
Takata, T., & Stevenson, D. J. 1996, Icarus, 123, 404
Takeda, H., Matsuda, T., Sawada, K., & Hayashi, C. 1985, Prog. Theor. Phys., 74, 272
Tanaka, H., Takeuchi, T., & Ward, W. R. 2002, ApJ, 565, 1257
Tremaine, S. 1991, Icarus, 89, 85
Ward, W. R. 1975, AJ, 80, 64
———. 1986, Icarus, 67, 164
———. 1989, ApJ, 336, 526
———. 1993, Icarus, 106, 274
———. 1996, in ASP Conf. Ser. 107, Completing the Inventory of the Solar System, ed. T. W. Rettig & J. M. Hahn (San Francisco: ASP), 337
Ward, W. R. 1997, Icarus, 126, 261
Ward, W. R., & Canup, R. M. 2000, Lunar Planet. Sci. Conf., 31, 2050
———. 2002, Paper presented at Jupiter Conference, Boulder CO (http://lasp.colorado.edu/jupiter)
Ward, W. R., Columbo, G., & Franklin, F. A. 1976, Icarus, 28, 441
Ward, W. R., & Hahn, J. M. 2000, in Protostars and Planets IV, ed. V. Mannings, A. P. Boss, & S. S. Russell (Tucson: Univ. Arizona Press), 1135
Ward, W. R., & Hamilton, D. 2002, in "Eurojove": Jupiter after Galileo and Cassini, ed. B. Battrick (ESA SP-510; Garching: ESA), in press
Ward, W. R., & Hourigan, K. 1989, ApJ, 347, 490
Weidenschilling, S. J., & Cuzzi, J. N. 1993, in Protostars and Planets III, ed. E. H. Levy & J. I. Lunine (Tucson: Univ. Arizona Press), 1031
Whipple, F. 1972, in From Plasma to Planet, ed. A. Elvins (New York: Wiley), 211
Yoder, C. F., & Peale, S. J. 1981, Icarus, 47, 1